Coordination Chemistry Reviews, 112 (1992) 131–168
Elsevier Science Publishers B.V., Amsterdam

Aluminium and gallium alkyls and their derivatives: spectroscopic and laser pyrolysis studies of metal deposition precursors

Douglas K. Russell
Department of Chemistry, University of Leicester, Leicester LE1 7RH (U.K.)

(Received 3 May 1991)

CONTENTS

A. INTRODUCTION AND BACKGROUND

One justification frequently used for the "blue skies" nature of much academic research is the unpredictability of the development of technology—one simply cannot foretell whether the results of one's work will be useful ten or fifty years from now. While many of us would be tempted to cite the theory of relativity or the invention of lasers in this kind of context, there are many such examples from the realms of chemistry. It would have been difficult to anticipate just a quarter of a century ago, for example, that the pyrolysis of trimethyl gallium—a pyrophoric, moisture-sensitive, and highly toxic volatile liquid—would assume a central role in the production of one of the most promising materials of the late twentieth century, namely gallium arsenide. Yet today, there are highly profitable chemical companies in the U.K. and

0010-8545/92/$15.00

elsewhere whose sole raison d'être is in the production of highly pure trimethyl gallium and similar compounds for use in the production of compound semi-conductor devices. Naturally, this sudden elevation to commercial status has initiated a flurry of related scientific activity. In this review, I shall describe the contribution of my own laboratory to this work. In common with a number of other investigators, we have applied more sophisticated modern experimental techniques in a re-examination of earlier work, sometimes with rather unexpected results.

In the following section, I shall briefly describe the background to this work. This features a description of the technologies involved, a brief mention of some of the chemical investigations of other workers, and a few somewhat subjective observations on problems currently in need of solution. There then follows a section describing the often novel methods used in our own investigations, principally that of infrared laser-powered homogeneous pyrolysis. The main section of this review contains descriptions of the investigations carried out thus far. This is necessarily sub-divided in a rather arbitrary way, since the results of one experiment often shed light on the interpretation of another; moreover, the whole area is the subject of intense current activity, and some of the results must therefore be regarded as provisional. Finally, I draw together some conclusions from the work, and provide an indication of developments expected in the immediate future.

Note on nomenclature. The names commonly used in the semi-conductor industry for many of the compounds discussed here are not those preferred by the International Union of Pure and Applied Chemistry; moreover, the materials are widely referred to by acronyms of the non-systematic name. Thus dimethylalane, Me_2AlH, is universally dimethyl aluminium hydride, DMAlH or DMAH; triethylgallane, Et_3Ga, is triethyl gallium, TEGa or TEG. A list of such abbreviations, including isotopic variants, is given in the Appendix. Furthermore, the chemistry of these materials is considerably complicated by the widespread occurrence of bridged dimeric, trimeric and higher oligomeric forms, often co-existent; while this fact is in large part responsible for their fascinating behaviour, it does render an accurate description of the precise nature of the materials something of a mouthful. For these reasons, although I shall attempt to use systematic names where precision dictates, I make no apology for frequent lapses into the argot of the industry.

B. THE CHEMISTRY OF THE SEMI-CONDUCTOR INDUSTRY

A wide-ranging description of the more chemical side of the manufacture of semi-conductor devices is provided by the book edited by Moss and Ledwith [1]. The particular aspect of interest here, namely the process of metal organic chemical vapour deposition (MOCVD, see the note on terminology in the Appendix), is superbly described in the recent book by Stringfellow [2]. The reader interested in the more technical aspects of the applications of the reactions described here is

referred to these works. Here I shall provide only a very brief description of the design of reactors in common use, in order to provide a framework within which to set the chemistry in context.

A typical MOCVD arrangement for the production of GaAs or other compound semi-conductor materials is schematically illustrated in Fig. 1. TMGa vapour is entrained in a carrier gas (usually H_2), mixed with AsH_3, and transported to the reaction chamber. Reactor pressures depend on the precise requirements, but may vary between atmospheric and a few torr (1 torr = 1 mm Hg = 133.3 N m^{-2}). The gas mixture is directed by a system of baffles over a substrate mounted on a graphite block: this is inductively heated by rf coils. At temperatures above 600 °C, this system produces epitaxial growth of highly pure GaAs. The stoichiometry of this reaction, first discovered by Manasevit in 1968 [3], is generally represented as

$$Me_3Ga + AsH_3 \rightarrow GaAs + 3CH_4 \quad (1)$$

Although a great deal is known about the requirements for the success of (1) in terms of purity of starting materials, temperature, pressure and flow conditions, and optimal reactor design, this has by and large been acquired in an empirical fashion. More recently, however, systematic investigations of processes such as (1) have been initiated. In order to disentangle the contributions of various components (homogeneous versus heterogeneous reactions, radical versus intramolecular processes, initiation by TMGa versus AlH_3, etc.), a whole battery of modern techniques has been brought to bear. These include mass spectrometry of reaction products, highly sensitive spectroscopic techniques for the detection of short-lived intermediates, and the chemist's traditional armoury of radical trapping, isotope labelling, and kinetic studies. More details of these investigations are provided in the discussions of individual systems below, but it is useful to provide a general view of the methods adopted in order to emphasise the unique features of our own work.

The traditional approach to the study of the MOCVD process has been the examination of the rate of production and quality of films deposited as a function

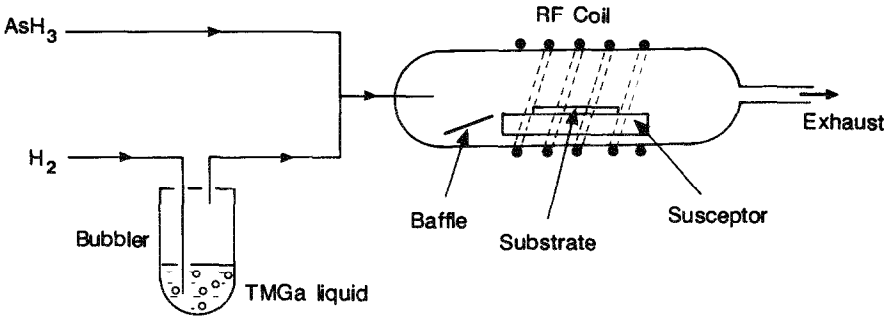

Fig. 1. Schematic MOCVD arrangement for the production of GaAs. In practice, there would be many more inlet lines, usually provided with automated switching for the production of devices.

of a number of variables—nature of the starting materials, temperature, pressure, flow rate, etc. This certainly provides the information most directly related to optimisation of the process, but yields very little by way of mechanistic detail. More recent studies have attempted to isolate single contributory factors. A good example of this is provided by a number of recent studies of the pyrolysis of TMGa alone, since it is widely accepted that bond homolysis in TMGa is the initial step involved in (1). Thus the pyrolysis has been studied in the presence of 1,4-cyclohexadiene as a radical trap [4], Me radicals have been detected directly using the highly sensitive IR tunable diode laser spectroscopy [5], and the physical and chemical effects of various carrier gases (H_2, D_2, N_2, and He) have been investigated [6]. However, even this kind of study is fraught with difficulty. This is well illustrated by studies of the pyrolysis of TEGa, widely used as an alternative Ga precursor to TMGa in GaAs production; among the 10 or so classical investigations, opinion has been divided on the relative importance of radical and β-elimination mechanisms [7]. Our own work is quite unambiguous on this point, as described below. The principal reason for this is that our work, almost uniquely, has provided information on the fate of the metal-containing fragments in pyrolysis reactions, whereas other workers have been obliged to make deductions from observed hydrocarbon products and the composition of the metal film ultimately deposited. This point is discussed in more detail in the Experimental section below.

C. EXPERIMENTAL METHODOLOGIES

The principal drawback of the usual pyrolysis methods for the study of reactions such as (1) paradoxically arises from the very same source as its practical utility, namely that the deposition of solid material provides a highly auto-catalytic surface for further reaction. This has been particularly clearly illustrated by Ashworth et al. in a closely related system, the oxidation of tetramethyltin, used in the production of tin oxide [8]:

$$SnMe_4 + O_2 \rightarrow SnO_2 + CO,\ CO_2,\ \text{etc.} \qquad (2)$$

Here, the reaction follows zero-order kinetics under all circumstances, clearly indicating an oxidation catalyzed by the SnO_2 surface. This kind of process makes it almost impossible to ensure complete elimination of heterogeneous reactions, since the greatly reduced activation energy of heterogeneous dissociation processes normally leads to domination by the latter. A second drawback of conventional hot-wall pyrolysis is that many of the primary products of pyrolysis, especially free radicals, are less stable than the starting materials. This means that one must resort to deduction of reaction mechanisms from the final products, usually hydrocarbons and deposited materials, which can often be misleading at best. There have, of course, been exceptions to this: for example, Me radicals have been detected in the MOCVD of TMGa [5]. By and large, however, primary and intermediate products, particularly

those containing the deposited elements, have not been observed. Both these problems are circumvented by the method of infrared laser powered homogeneous pyrolosis (IR LPHP), which is used almost exclusively in our work. Since the benefits of this technique are central to the studies below, it is now described in outline. For a more detailed discussion of the method and its application in other fields, the interested reader is directed to a recent review [9].

The essentials of the IR LPHP technique are illustrated in Fig. 2. A mixture of the gas or gases under study and an inert IR absorber (usually SF_6) at pressures of a few torr is contained in a static pyrex cell. This has a volume of approximately 50 cm^3, so that very small quantities of material are needed. The cell is fitted with a filling port and sometimes a detachable side-arm for sample isolation and manipulation. The ends of the cell are enclosed by a pair of ZnSe windows: this material is crucial to the success of the work described here, since the cheaper alkali halides are too hygroscopic and lead to extensive hydrolysis. For moderately volatile precursors (vapour pressures <1 torr), the liquid starting material may be retained in a cylindrical hollow in the cell, illustrated in Fig. 2. The cell is then subjected to the output (up to 50 W) of a free-running CO_2 IR laser. Absorption of the laser radiation by the SF_6 is followed by very rapid intra- and intermolecular energy conversion, and the release of heat into the gas mixture. As has been shown by a number of workers [10,11], this generates a highly inhomogeneous temperature profile, in which the centre of the cell may be heated as high as 1500 K (at which temperature pyrolysis of the SF_6 photosensitiser sets in), but the cell walls remain at room temperature. Changes of composition may be monitored by any convenient method: although some workers have utilised mass spectrometry [12] or gas chromatography [13], we

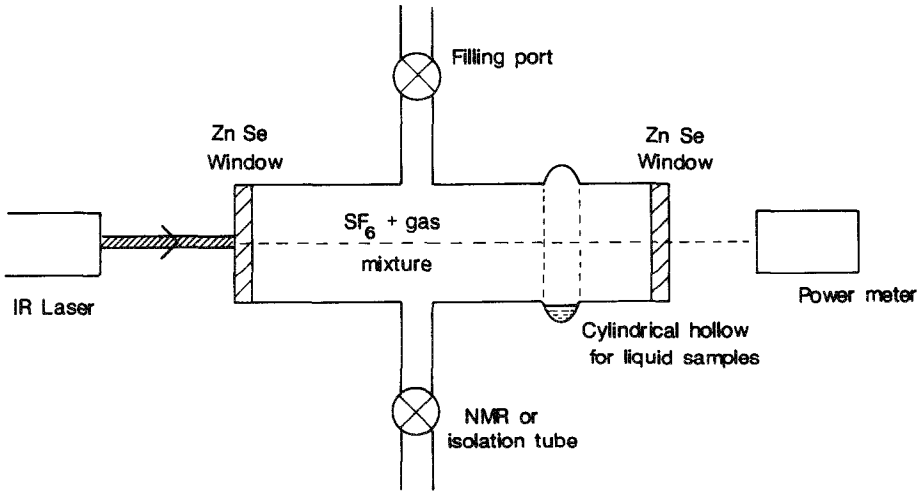

Fig. 2. Essentials of the IR LPHP technique. The ZnSe windows provide access for FTIR monitoring as well as for IR laser irradiation.

have preferred the non-invasive Fourier transform infrared spectroscopy (FTIR). This latter method is particularly convenient, conferring benefits of speed and ease of computer manipulation. Further analytical techniques (principally NMR) may be applied to products collected and purified in the side tube.

As described above, the maintenance of the cell walls at room temperature ensures the complete elimination of surface-initiated reaction. This has been amply attested, not only by our own work, but in the more than 200 other publications using the technique [9]. The second benefit, that of preservation of unstable intermediates, has been rather less widely appreciated. This arises essentially since the dissociation of starting material in the hot zone is followed by rapid ejection of products into cooler regions of the cell. If these products are less volatile, they may condense on the cold cell walls, and be examined at leisure. If they are reactive, such as free radicals, they may be trapped chemically or physically (e.g. in a low-temperature matrix). All of these points are illustrated in the investigations below.

As mentioned above, analysis of reaction products has been carried out using chiefly IR and NMR spectroscopy. Many of the products observed are quite novel, and this has therefore necessitated a number of spectroscopic investigations. These are also described below.

D. INVESTIGATIONS, RESULTS, AND COMMENTS

In this section, I shall present the results of the majority of investigations carried out in my laboratory over the past three years. Since our approach to the study of the reactions is somewhat novel, particularly amongst the MOCVD community, I shall describe the experimental procedures in some detail. This is, I believe, justified by the evolution of an experimental protocol which has succeeded in elucidating mechanisms of reaction in greater detail than hitherto. Although some conclusions relating to individual studies may be given at this stage, it is already very evident that a more valuable outcome of the work will be the evaluation of trends and comparisons between systems. For this reason, the majority of the discussion of the overall significance of the results is deferred until the last section. In order to avoid a surfeit of figures, FTIR and NMR spectra are normally presented only where they have not previously been published: the reader is referred to the original works for details of the spectroscopic observations.

(i) Trimethyl aluminium, TMAl

The study of the pyrolysis of TMAl occupies a significant position in our work as the first demonstrated example of the quite unique advantages of the IR LPHP method in the study of the chemistry of MOCVD processes [14]. It also provided a relatively simple system for the evolution of experimental procedures for the study of the mechanism of the pyrolysis of MOCVD precursors. For these reasons, the

experimental work carried out for this system is described in rather greater detail than would be common in a review of this sort. As indicated by both Moss and Ledwith [1] and Stringfellow [2], a considerable amount of work had already been done on this reaction. This has mostly taken the form of examination of the hydrocarbon products (largely methane, with some ethane, ethene and higher hydrocarbons at elevated temperatures) under various regimes of temperature, pressure, flow conditions, and nature of carrier gas. Apart from phenomenological studies of the quality of aluminium deposited, there have been no previous attempts to investigate the fate of aluminium-containing species. These studies provide a classic example of the extreme sensitivity of the reaction to surface conditions, and the dangers arising from insufficient attention to this problem. Two papers published as recently as 1986 have reported activation energies for the pyrolysis as divergent as 158.8 kJ mol^{-1} [15] and 38 kJ mol^{-1} [16], both claiming to have eliminated heterogeneous contributions!

FTIR spectra of a mixture of SF_6 (10 torr) and TMAl (2 torr) before and after laser pyrolysis are shown in Fig. 3. The laser power used here was 8 W; as described above, temperatures are not precisely defined in this technique, but indications are

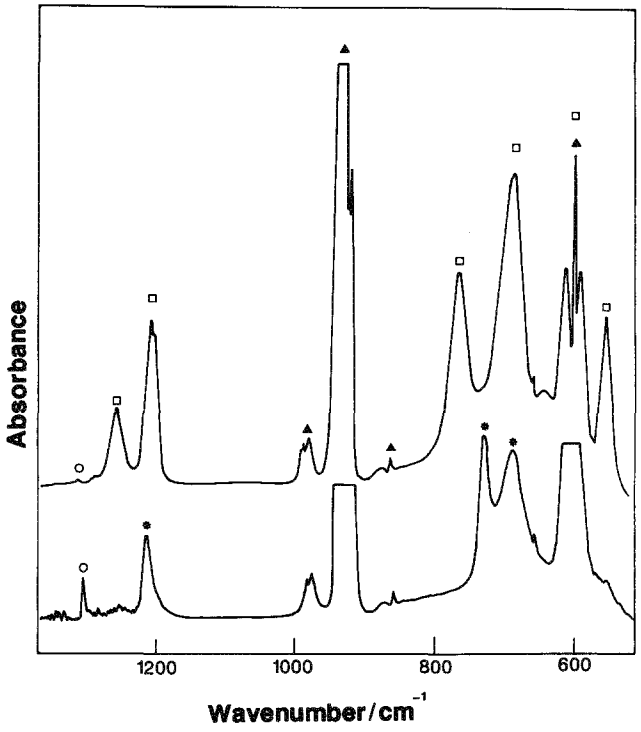

Fig. 3. FTIR spectra of a mixture of SF_6 (10 torr) and TMAl (2 torr) before (top) and after (bottom) exposure to 8 W IR laser irradiation for 2 min. Features identified arise from SF_6 (▲), TMAl (□), CH_4 (○), and DMAlF (★).

that this provides a maximum temperature of 800–900 K. At this temperature, complete loss of the TMAl starting material (as indicated by disappearance of the bridging CH_3 symmetric deformation near 1250 cm^{-1}) occurs over a period of a few minutes. Also evident from Fig. 3 are the production of methane (sharp Q-branches near 1310 and 3100 cm^{-1}), and considerable changes in the region associated with the skeletal vibrations of TMAl around 700 cm^{-1}. In particular, the strong band near 770 cm^{-1} (associated with rocking vibrations of the bridging CH_3 groups) disappears, to be replaced by an equally intense band at 740 cm^{-1}. At the same time, the feature at 560 cm^{-1} (the symmetric stretching of the $AlMe_2$ units) becomes very much weaker in intensity. Other changes in the spectrum are obscured by overlap with strong SF_6 or residual TMAl features. To eliminate these, the pyrolysis products were condensed into a side tube at 77 K, followed by pumping at 196 K (at which temperature both SF_6 and CH_4 are removed) and re-expansion into the gas cell. The product proved to be a highly viscous, slightly volatile liquid whose IR spectrum (both vapour and liquid) is shown in Figs. 2 and 3 of ref. 14.

Further analysis was attempted using Raman spectroscopy, mass spectrometry, elemental analysis, and NMR methods: in this case, we also carried out cryoscopic measurements of relative molecular mass. None of the first three proved particularly helpful—Raman spectroscopy provided little information not available from IR studies, mass spectrometry of organoaluminium compounds is notoriously difficult (see, for example, ref. 17), and the small quantities available rendered results of compositional analysis too imprecise to be of real value. However, NMR (^1H, ^{19}F, and ^{13}C) spectroscopy proved to be highly informative, and, along with the FTIR spectroscopy, has become established as the principal analytical technique in the investigations described here. The gaseous (or volatile liquid) products were condensed into an NMR tube attached directly to the pyrolysis cell (see Fig. 2), and solvent (in this case carefully dried $CDCl_3$) added by subsequent condensation. The room-temperature ^1H NMR spectrum consisted of a broad singlet at δH −0.637 ppm; this showed no change on cooling to the freezing point of the solvent, but addition of a small quantity (< 5%) of TMAl produced a 1:2:1 triplet with a splitting of 4.50 Hz. The ^{19}F spectrum consisted of a single broad feature at δF −144.9 ppm (referred to $CFCl_3$); using CF_3CH_2OH as an external reference, the ^1H:^{19}F ratio was estimated to be 6.5 (±10%). Freezing point depression measurements in CCl_4 yielded a RMM of 324 (±5%).

These observations are consistent with the identification of the product as tetrameric dimethyl aluminium fluoride (DMAlF), $\{Me_2AlF\}_4$. This suggests that the dimethyl aluminium radical, Me_2Al, is a significant intermediate in the pyrolysis system, and the fluoride product is a result of abstraction of F atoms from the SF_6 by this radical. (This, incidentally, provides one of the few instances of chemical participation by the photosensitiser in IR LPHP; the other recorded examples involve silicon species [18], and this is entirely consistent with the known exceptional strengths of Al–F and Si–F bonds [19].) In order to test this hypothesis, we attempted

to trap the Me_2Al with other species. An obvious choice was CCl_4: the reaction of TMAl with CCl_4 is well known [20], and CCl_4 alone proved to be thermally stable under our LPHP conditions. FTIR spectra of SF_6/TMAl/CCl_4 mixtures are shown in Fig. 4 of ref. 14. In this case, the observed changes were entirely consistent with formation of the expected Me_2AlCl product [21], and this was confirmed by ^1H NMR [22].

These observations are consistent with the sequence of reactions

$$Me_3Al \rightarrow Me_2Al + Me \quad (3)$$

$$Me_2Al + SF_6 \rightarrow Me_2AlF + SF_5 \quad (4)$$

or

$$Me_2Al + CCl_4 \rightarrow Me_2AlCl + CCl_3 \quad (5)$$

However, almost as many questions are raised as answered by this mechanism. It is well-known, of course, that TMAl is almost entirely dimeric at room temperature, with almost complete dissociation into monomer at temperatures around 100–150 °C [23]. Is dimer–monomer dissociation rate-limiting in our system, or is it the Al–C bond homolysis of the monomer, as suggested in reaction (3) above? Secondly, what is the fate of the Me radicals, which are presumably responsible for the hydrocarbon products (entirely CH_4 in our system, but partly higher hydrocarbons in others)? Third, it is well-known that MOCVD from TMAl produces aluminium badly contaminated by unwanted carbon; is there anything in our mechanism which suggests itself as a source of this carbon, or must this be attributed to surface processes? Finally, of course, what is the extent of the significance of gas-phase reactions in the overall MOCVD process? Some of these questions have been answered, while others are the subject of current investigations.

In order to address the first point, we have examined the FTIR spectra of both TMAl/SF_6 and dTMAl/SF_6 mixtures under the conditions of IR LPHP [24]. FTIR spectra of these mixtures, both in the absence and presence of IR laser radiation, are shown in ref.24. Changes in the spectra at laser powers below that required for significant pyrolysis of the TMAl are entirely consistent with almost complete dissociation into monomer units, on comparison with reported spectra of monomeric TMAl isolated in inert matrices [25]. This observation confirms that dimer dissociation is not rate-limiting. In fact, this observation represents the first report of the IR spectrum of monomeric TMAl in the gas phase: we therefore undertook a complete analysis of these spectra, including normal coordinate analysis and comparison with ab initio calculations of vibrational frequencies and intensities. For comparison, we also included a similar study of TMGa and dTMGa in this work. The results of this work have a considerable bearing on the mechanism of pyrolysis of TMAl, especially in comparison with the superficially similar TMGa, and will be discussed at appropriate points below. They also correct some previous misconceptions about organo-

aluminium IR spectra: the most significant of these is that vibrations associated with stretching of the $AlMe_2$ unit, particularly the asymmetric stretch, have been shown to be remarkably weak, whereas many previous analyses have assumed them to be among the strongest in the spectrum [25].

We have carried out a thorough study in an attempt to answer the second point raised above, and also some others related to it. We have first confirmed that Me radicals do indeed feature in the gas-phase reaction by isolating the products of pyrolysis in an adamantane matrix, and investigating the resultant ESR spectrum [26]. This is shown in Fig. 4.

The very strong 1:3:3:1 quartet is easily identified as arising from the Me radical; there is, in addition, a weaker spectrum which has yet to be positively identified, but is almost certainly an aluminium-containing radical, perhaps $MeAl(CH_2)H$ arising from re-arrangement of Me_2Al. This confirms the earlier detection of Me radicals by Squire et al. using tunable diode laser IR spectroscopy, although their study was of surface-mediated reaction [27].

In conventional MOCVD systems, the slightly volatile organometallic reagents are generally carried in a stream of hydrogen, and although some previous studies

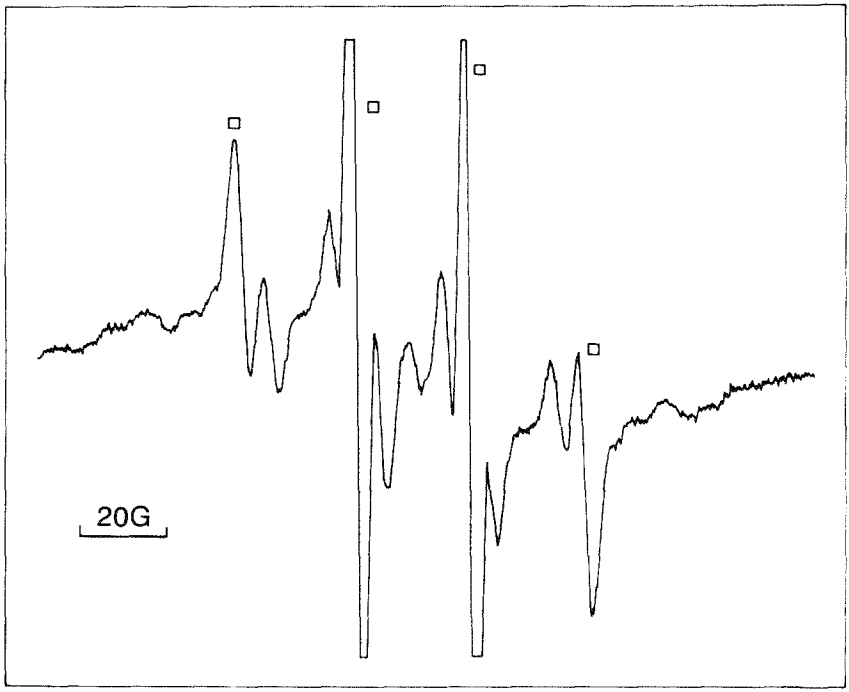

Fig. 4. X-Band ESR spectrum of the products of pyrolysis of TMAl trapped in an adamantane matrix. The strong 1:3:3:1 quartet marked □ arises from CH_3 radicals; the remaining weaker signals have yet to be identified.

have attempted to determine whether this plays a chemical part in the overall process, it is still not clear what this is. We have therefore studied the IR LPHP of both TMAl and dTMAl in the presence of hydrogen and deuterium. Although physical constraints of the IR LPHP technique limit the range of H_2:TMAl ratios available to a maximum of about 10:1, it is very apparent that, by and large, hydrogen does not play a significant role in the homogeneous pyrolysis. This is in some contrast to the studies of earlier workers [15, 16], who have suggested that the use of hydrogen as a carrier gas (in place of inert nitrogen or helium) both increases the production of methane and decreases the activation energy of the pyrolysis. We believe this is an example of the dominant effect of heterogeneous reactions, even under circumstances where one would normally believe them to be negligible. The only circumstance under which we have observed chemical effects of added hydrogen comes from observations of the dTMAl/H_2 mixture, where very small quantities of CD_3H are observed. These observations are readily rationalised by the reactions

$$Me + H_2 \rightarrow CH_4 + H \tag{6}$$

$$Me + TMAl \rightarrow CH_4 + Me_2AlCH_2 \tag{7}$$

as competing reaction channels leading to methane formation from the methyl radical. Our normal coordinate analysis of the monomeric TMAl described above has led to the conclusion that the C–H bond in this compound is anomalously weak (some 1–2% weaker than in many other MMe_3 compounds, most significantly TMGa), and thus reaction (7) is favoured in the above scheme. The reactions are clearly finely balanced, since the small kinetic isotope effect of replacing TMAl by dTMAl is sufficient to tilt the energetics slightly towards reaction with hydrogen. This observation is in marked contrast with the case of TMGa (see below).

This observation is also quite relevant to the third point raised above, namely the origin of the carbon contamination in the MOCVD of aluminium. The Al–CH_2 bond in the radical resulting from hydrogen atom-abstraction has been shown to have considerable double bond character, as indicated by ab initio calculations carried out on this [28] and other similar systems [29]. Thus the loss of this carbon centre would require a rather greater activation energy than that of methyl units, leading to retention of carbon in deposited aluminium. While this conclusion is conjectural, and is obviously dependent on a considerable homogeneous contribution to the MOCVD process, it is certainly consistent with the observations to date. One route to test this hypothesis out is to carry out MOCVD studies of the isotopic precursors, and this is currently under study [30].

The final point is the most difficult one, namely the contribution of the gas-phase processes under normal MOCVD conditions. The only way in which this can be answered definitively is to extract reliable kinetic parameters for all possible homogeneous and heterogeneous reactions, and to model the overall process. As described above, conventional kinetic studies are too often dogged by uncertainties,

and unfortunately the static IR LPHP method does not lend itself too readily to kinetic studies. However, pulsed IR LPHP techniques can provide reliable kinetic data [9], and this is one possible way forward.

(ii) Dimethyl aluminium hydride, DMAlH

One of the principal problems in the production of aluminium-containing semiconductors is heavy incorporation of carbon: this has a deleterious effect, since the resultant deep electron traps significantly reduce electron mobility [2]. The traditional aluminium precursor has been TMAl, and it is widely accepted that it is the methyl radicals produced which are the culprit here. However, as described above, agreement is less universal on the precise manner in which this occurs. Some have suggested that incomplete elimination of methyl groups from the metal centre in heterogeneous reactions may be the cause; our own experiments (see above) suggest that methyl radical attack on the parent, resulting in the production of a strong $Al{-}CH_2$ bond, may be significant. Whatever the origin of the problem, there have been strenuous efforts to circumvent it by identifying alternative aluminium-containing precursors. Investigations of two possible candidates are described in this section and in Sect. D.(iv).

Dimethyl aluminium hydride (dimethylalane, DMAlH) is a highly viscous, slightly volatile (2 torr at room temperature) liquid, first prepared in 1953 by Wartik and Schlesinger [31]. Its IR spectrum was described in two publications by Hoffman et al. [32,33], and the latter work provided a fairly detailed analysis, although deuterated species were not investigated. In our work, we wished to investigate isotopically substituted DMAlH (principally $(CH_3)_2AlD$, DMAlD and $(CD_3)_2AlH$, d_6-DMAlH), and we therefore undertook an examination of the IR spectra of these species. This revealed a number of inconsistencies in the assignments of Schrötter and Hoffman [33], and, since the correct identification of the species present was crucial to our interpretations, we carried out a complete analysis of these spectra. This has been reported elsewhere [34], and the results are summarised here.

(a) The vapour of DMAlH is largely dimeric through hydrogen bridging bonds (i.e. it is $Me_2Al(\mu H)_2AlMe_2$) at room temperature. This conclusion is in contrast with those of earlier workers [31–33], who deduced that the vapour is largely trimeric, based on its behaviour in solution, and on erroneous identifications in the IR spectra. Electron diffraction studies, on the other hand, have shown that the vapour is certainly entirely dimeric above 150 °C [35]. This conclusion is of some importance in calculations of stoichiometry in MOCVD. Attempts to detect the monomer of DMAlH in the manner described above for TMAl were totally unsuccessful, resulting only in complete pyrolysis above a threshhold temperature; we therefore conclude that it is probably reaction of the dimer species which is rate-limiting in DMAlH, as opposed to the monomer as in TMAl.

(b) In the dimeric form, the Al–C bond strength is slightly weaker (2%) than that in monomeric TMAl, but the C–H bond strength is substantially the same.

(c) Exchange of bridging hydrogen is rapid in the vapour, even at room temperature. This was demonstrated by the observation of a statistical (1:2:1) mixture of the possible dimeric bridged forms $(\mu H)_2$, $(\mu H)(\mu D)$, and $(\mu D)_2$ in an initial 1:1 mixture of the vapours of DMAlH and DMAlD. This kind of exchange is, of course, very familiar in the liquid phase through variable-temperature NMR studies, but its demonstration in the gas phase has been hampered by inadequate understanding of IR spectra. The observation of bridging H exchange in the gas phase is of some importance, since it may provide an insight into the mechanism of pyrolysis; it suggests, for example, that Al–H–Al bridging bonds may indeed break and reform, even in the gas phase. The identification of the heterobridged form was particularly important, since it appeared in our IR LPHP studies.

(d) A strong peak appearing in all forms between 800 and 850 cm^{-1} (depending on isotopic form) has been correctly identified for the first time as the $AlMe_2$ rocking vibration. This has been very helpful in our work, since its highly characteristic doublet appearance, and dependence on the mass of the bridging units, has proved invaluable in identifying a number of $Me_2Al(\mu H)(\mu X)AlMe_2$ species.

Preliminary studies have shown that DMAlH provides aluminium-based semiconductors of much reduced carbon incorporation [36], and we have therefore undertaken an extensive study of the IR LPHP of this species [37]. FTIR spectra of DMAlH/SF_6 mixtures before and after brief IR LPHP are shown in Fig. 5.

The principle changes observed are loss of the broad bands near 1800 and 800 cm^{-1}, which are assignable to Al–H stretches in the trimeric form of DMAlH [34], minor changes in the bands around 1200–1400 cm^{-1} (Al–H stretches in dimeric DMAlH), a new weak shoulder near 750 cm^{-1}, characteristic of Al–F–Al bridged species [14], and loss of the strong doublet near 850 cm^{-1}, with a simultaneous growth of a similar doublet at 816 cm^{-1}. This doublet near 800 cm^{-1} is highly characteristic of the system $Me_2Al(\mu H)(\mu X)AlMe_2$, appearing at 851 cm^{-1} (X = H [34]), 810 cm^{-1} (X = D [34]), or 815 cm^{-1} (X = Me [38]). These observations are consistent with the identification of the major product as the hetero-bridged $Me_2Al(\mu H)(\mu F)AlMe_2$. This was confirmed by ^1H and ^{19}F NMR of the product isolated in the manner described for DMAlF above. At −70 °C, the ^1H spectrum showed two broad singlets in the region characteristic of Al–H protons at δH 2.66 and 3.64 ppm, and three resonances in the region of Al–Me protons at δH −0.41, −0.47, and −0.52 ppm. The first of these in each case arises from unreacted DMAlH, and the last of the methyl group resonances from DMAlF [14]. At the same temperature, the ^{19}F spectrum showed two broad singlets at δF −144.37 and −142.75 ppm, the first again being assigned to DMAlF [14]. The remaining resonances are consistent with the identification of the mixed bridged dimer. At room temperature, all ^1H NMR signals shifted and broadened, and there was evidence of exchange of methyl groups: on the other hand, there was no evidence of exchange

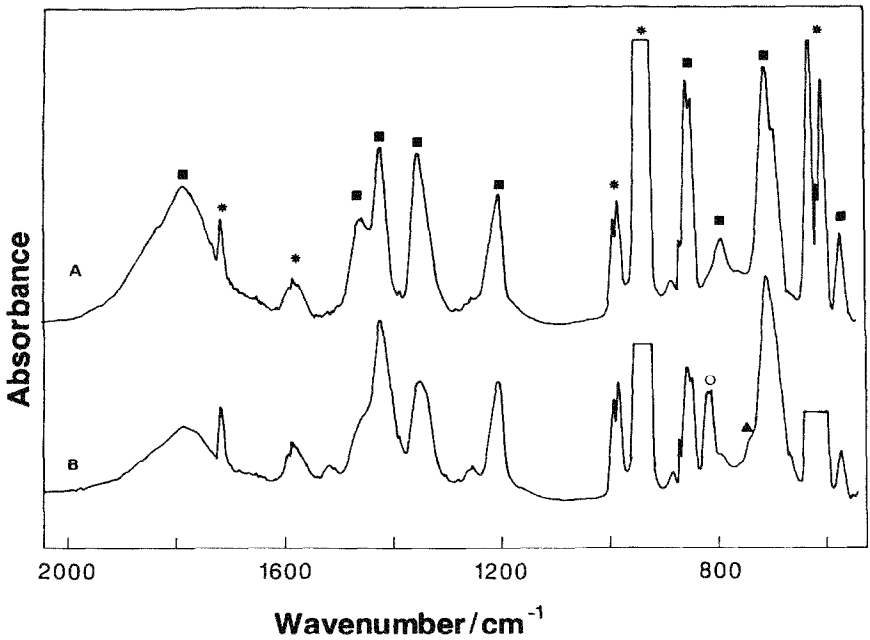

Fig. 5. FTIR spectra of a mixture of SF_6 (10 torr) and DMAlH (2 torr) before (top) and after (bottom) exposure to 5 W IR laser irradiation for 17 s. Features identified arise from SF_6 (★), DMAlH (■), and the $AlMe_2$ rocking (○) and Al–F stretching (▲) of the mixed bridged $Me_2Al(\mu H)(\mu F)AlMe_2$.

of the bridging atoms. This is in contrast to the observation of rapid exchange between bridging hydrogen atoms in gaseous DMAlH, and is presumably related to the known great strength of the Al–F–Al bridging bond.

The observation of this species is of considerable interest in its own right, since it provides the first example of an isolatable organoaluminium species bridged through two different atomic moieties (there are, of course, many examples of such hetero-bridged compounds with large molecular bridging units [39]). Moreover, it is the first reported instance of a hetero-bridged species in which one of the bridging units is F. The reason for this is the great strength of the Al–F–Al bridging bond: indeed, attempts to synthesise this species by mixing DMAlH and DMAlF were less successful, resulting in a very small yield [40]. We return to the mode of formation of the product below.

It will be noted that the brief IR LPHP of DMAlH produces little or no methane (compare Figs. 5 and 3), and it would be tempting to correlate this with the decreased carbon content using DMAlH as a source in MOCVD. However, prolonged or more vigorous IR LPHP does produce methane albeit in rather lower yield (approximately 50%) than from TMAl. In order to investigate the origin of this methane, we have subjected the isotopic versions DMAlD and d_6-DMAlH to IR LPHP; in the former case, the only isotopic methane produced was CH_3D, and

in the latter CD_3H. In all cases, the only identifiable aluminium-containing product was the appropriate isotopic DMAlF. Finally, we have investigated the effect of adding hydrogen or deuterium, which is widely used as a carrier gas in MOCVD. In all cases but one, no new products were observed. The exception to this came from the IR LPHP of the mixture of DMAlD with hydrogen, where the hetero-bridged $Me_2Al(\mu H)(\mu D)AlMe_2$ was produced [37].

From our work on the IR LPHP of TMAl [14], it would appear that the production of DMAlF arises from fluorine-abstraction from SF_6 by Me_2Al radicals, and any mechanism proposed must incorporate these. There remain several unresolved aspects of the mechanism of pyrolysis of DMAlH, but a scheme consistent with most of the observations is as follows:

$$Me_2Al(\mu H)_2AlMe_2 \rightarrow 2Me_2AlH \quad (8)$$

$$Me_2AlH \rightarrow Me + MeAlH \quad (9)$$

$$Me + Me_2AlH \rightarrow CH_4 + Me_2Al \quad (10)$$

$$Me_2Al + SF_6 \rightarrow Me_2AlF + SF_5 \quad (11)$$

$$Me_2Al + H_2 \rightarrow Me_2AlH + H \quad (12)$$

$$Me_2AlF + Me_2AlH \rightarrow Me_2Al(\mu H)(\mu F)AlMe_2 \quad (13)$$

with similar reactions, mutatis mutandis, for deuterated forms. As described above, monomeric Me_2AlH is not present in detectable quantities, and thus reaction (8) may be the rate-determining step. However, this is highly conjectural at this stage, and a concerted combination of reactions (8)–(10) is quite possible. The studies involving the production of isotopic methanes reveal that methyl radicals react exclusively with the aluminium-bound hydrogen atoms; the elimination of the equivalent of reaction (7) for TMAl is consistent with the reduction in carbon contamination. Reaction (11) yields Me_2AlF in a nascent (possibly monomeric) form; under conditions of short pyrolysis, this presumably interacts with excess DMAlH starting material to form the hetero-bridged product (13), whereas under longer pyrolysis, it simply co-condenses to yield the familiar trimeric or tetrameric fluoride [14]. This explains why the hetero-bridged species is produced under IR LPHP conditions, since dissociation of the strong Al–F–Al bonds is never required. Reaction (12) is required to rationalise the production of $Me_2Al(\mu H)(\mu D)AlMe_2$ in the co-pyrolysis of DMAlD and hydrogen. The non-observation of this product in the corresponding DMAlH + deuterium system can be ascribed to the kinetic isotope effect: our studies of many systems, significantly TMAl [14] and TMGa [41], have clearly shown that the overall chemistry is very delicately balanced, and kinetic isotope effects could be as large as a factor of 8 or 10 for reactions such as (12). The reduced importance of reaction (12) in the $TMAl/H_2$ pyrolysis is simply a temperature effect, since any Me_2AlH product would be very rapidly lost at the higher temperatures used in this

latter case. The principal observation not accounted for in the above scheme is the lack of any methane at early stages in mild pyrolysis. It may well be that there is an alternative mechanism of lower activation energy and Arrhenius A-factor, perhaps involving loss of molecular hydrogen with the formation of Me_2Al radicals; it should be noted that hydrogen is not detected by our methods.

(iii) Exchange reactions in aluminium and gallium precursors

Although there are uses for semi-conductor materials containing aluminium as the only Group III element [2], a more general and widespread application is in ternary compounds such as $Al_xGa_{1-x}As$ (usually known simply as AlGaAs). In these materials, the band gap can be tuned by variation of the stoichiometry without significantly altering the crystal structure, and this permits the epitaxial growth of heterostructures. MOCVD of these materials requires both aluminium and gallium precursors: unless both contain the same alkyl moieties, there is the possibility of exchange and the production of unwanted characteristics. Exchange reactions of groups between aluminium and gallium alkyls and their derivatives have been very widely studied in solution, principally using variable temperature ^1H, ^{13}C, or ^{27}Al NMR [42]. On the other hand, very little is known about the significance of such processes in the gas phase: our studies of the state of aggregation of DMAlH (see above) suggest that a different state of affairs may result from rather small shifts in what are evidently closely balanced driving forces. For this reason, we have carried out a study of exchange reactions involving TMAl, DMAlH, and TMGa, described in this section; in the next, we describe comparable studies using a second alternative Al precursor.

(a) TMAl + TMGa

Comparison of the FTIR spectrum of a mixture of TMAl and TMGa with a computer co-added spectrum of the two separate components reveals that no new products are formed at detectable concentrations. However, exchange of methyl groups certainly does occur, as indicated by the corresponding spectra using dTMAl and TMGa (Fig. 6). This is not surprising, but it does call into question the mechanisms of such processes proposed by some previous workers, who have suggested that the formation of monomers contained in solvent cages may be significant [43]. The spectrum of Fig. 6 is too heavily overlapped for a detailed analysis, but presumably consists of overlapping contributions of all possible isotopic combinations in statistical proportions.

(b) TMAl + DMAlH or DMAlD

As a preliminary to a study of DMAlH and TMGa, we have studied mixtures of TMAl and DMAlH; spectra of the mixture and a computer co-addition are shown in Fig. 7.

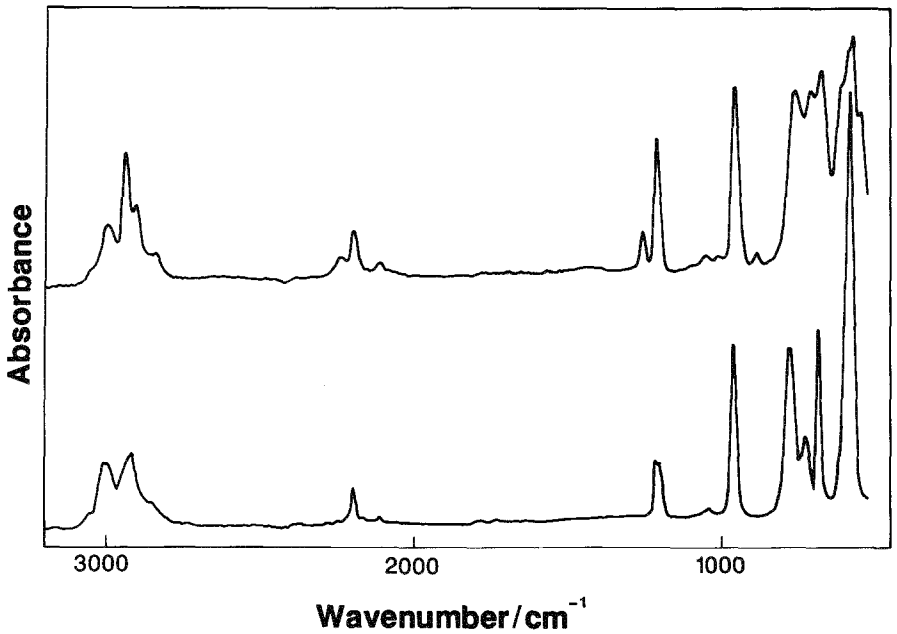

Fig. 6. FTIR spectrum of a 1:1 mixture of dTMAl and TMGa (top), and computer co-added spectra of the two components in the same ratio (bottom). Note the appearance of peaks arising from bridging methyl groups in TMAl near 1250 cm^{-1} in the upper spectrum, and of additional features in the C–H and C–D stretching regions near 3000 and 2200 cm^{-1}.

A number of crucial features are overlapped in this system, and we have therefore studied TMAl and DMAlD in addition; corresponding spectra are shown in Fig. 8. The principle changes evident from Fig. 7 are loss of the broad strong peak near 1800 cm^{-1} (due to the trimer of DMAlH), the almost complete replacement of the characteristic doublet at 851 cm^{-1} by a very similar peak at 815 cm^{-1}, and the partial disappearance of features arising from bridging methyl groups in dimeric TMAl (the symmetric methyl deformation at 1255 cm^{-1}, and the methyl rocking at 774 cm^{-1}). There are also less easily interpreted changes in the region of bridging Al–H vibrations in dimeric DMAlH between 1200 and 1450 cm^{-1}. These become clearer in the DMAlD + TMAl spectrum, where the Al–D vibrations are shifted away from the region of the methyl symmetric and asymmetric deformations, and are less subject to splitting by Fermi resonances [34]. Here it is apparent that both the symmetric Al–D stretch (at 1006 cm^{-1}) and its asymmetric counterpart (905 cm^{-1}) have been replaced by similar bands at slightly higher wavenumber (1038 and 945 cm^{-1} respectively). With an appropriate isotopic shift, this now can also be seen to be the pattern in the TMAl/DMAlH spectrum.

These observations are readily interpreted in terms of a mixture containing largely the hetero-bridged dimer $Me_2Al(\mu H)(\mu Me)AlMe_2$, with considerably smaller amounts of the homo-bridged starting materials and of mixed trimers. This certainly

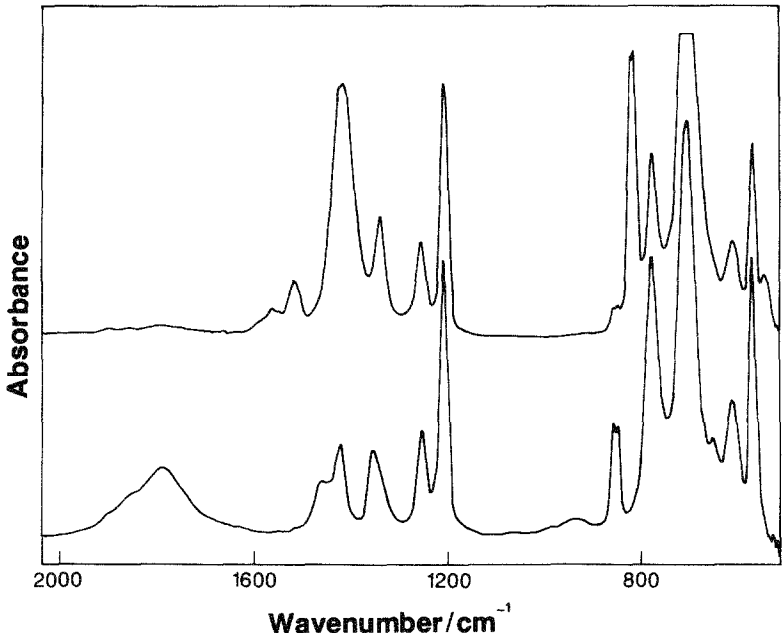

Fig. 7. FTIR spectrum of a 1:1 mixture of DMAlH and TMAl (top), and computer co-added spectra of the two components in the same ratio (bottom). Note the loss of the broad peak near 1800 cm^{-1} due to trimeric DMAlH, and the almost complete replacement of the $AlMe_2$ rocking peak of dimeric DMAlH near 850 cm^{-1} by a similar feature near 815 cm^{-1}.

accounts for the decrease of peaks ascribed to bridging methyl groups, the shifts in dimeric Al–H vibrations, and to the virtual disappearance of the trimeric Al–H bands. The most telling feature, however, is the band at 815 cm^{-1} in the DMAlH mixture: as we have shown elsewhere [34, 40], this feature is characteristic of the rocking motion of the $AlMe_2$ moiety in molecules containing the $(\mu H)(\mu X)AlMe_2$ unit, with the precise wavenumber depending largely on the mass of the second bridging species X. A normal coordinate analysis of the spectra of the dimeric hetero-bridged species (obtained by computer subtraction of residual starting material features from the spectra of the mixtures) has confirmed this hypothesis [44]. While the observation of this kind of mixed bridge species is not novel [45], the extent to which it predominates in the gas phase (>95%) was somewhat unexpected; presumably, the presence of a hetero-bridging group somewhat strengthens the Al–H bridging bond, and this contention is certainly supported by the force constants obtained in preliminary normal coordinate calculations [44].

(c) TMGa + DMAlH or DMAlD

As described above, we were also interested in the products of exchange reactions in mixtures used in the production of AlGaAs films. Figures 9 and 10 show computer-added and observed spectra of mixtures of TMGa and DMAlH or DMAlD.

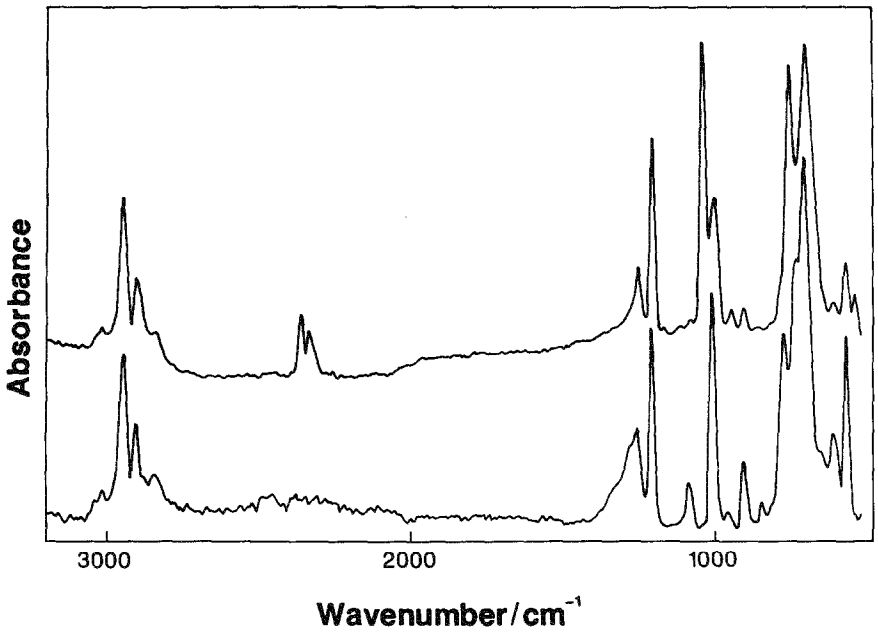

Fig. 8. As for Fig. 7 with DMAlD in place of DMAlH. The new strong feature near 1040 cm^{-1} arises from $Me_2Al(\mu D)(\mu Me)AlMe_2$; the doublet near 2300 cm^{-1} in the top spectrum arises from CO_2.

Once again, there are very marked changes. In particular, the characteristic $AlMe_2$ rocking vibration drops from 851 to 815 cm^{-1}, a new strong feature appears at 1280 cm^{-1}, the methyl symmetric bending at 1205 cm^{-1} acquires a pronounced broad shoulder on its low-frequency side, and the broad strong Al–H vibration at 1800 cm^{-1} weakens and shifts downwards. On inspection of the spectra of the exchange products (obtained by computer subtraction of those of the starting materials, see Figs. 9 and 10) and comparison with the published spectrum of DMGaH and the TMA/DMAlH mixture described above, it is apparent that the majority species in the mixture are DMGaH and the hetero-bridged $Me_2Al(\mu H)(\mu Me)AlMe_2$. This conclusion is borne out by the TMGa/DMAlD mixture. It is evident that migration of hydrogen groups from aluminium to gallium centres is rapid in the gas phase, with a corresponding increase in the number of methyl groups found in aluminium species. This is consistent with the greater electronegativity of gallium, and with our studies of $AlH_3 \cdot NMe_3 + TMGa$ mixtures described below. It also underlines once again the need to consider carefully gas-phase interactions when contemplating studies of pyrolysis mechanisms in such mixtures.

(iv) Exchange studies of trimethylamine alane and trialkylgallium compounds

As described in the section above, there is a considerable interest in alternative aluminium precursors, particularly those which contain fewer Al–Me bonds. The

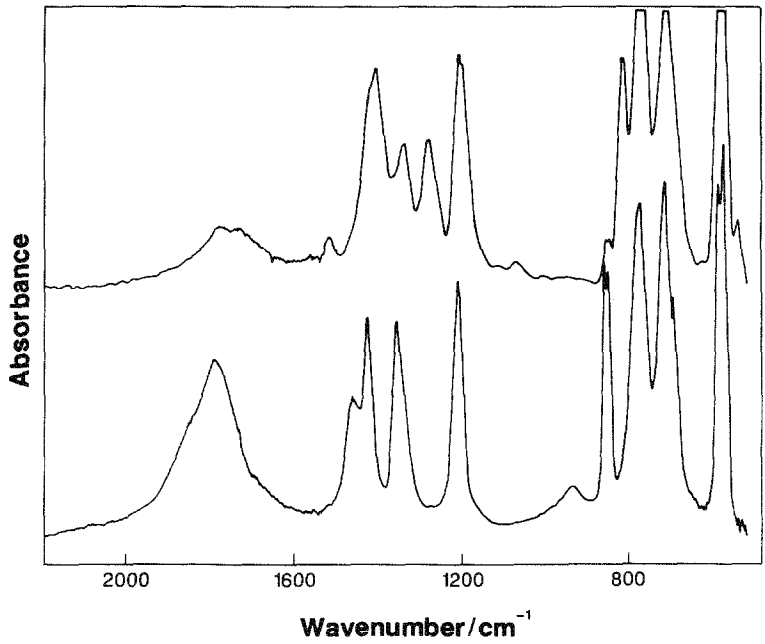

Fig. 9. As for Fig. 7, with TMGa in place of TMAl. As well as new features similar to those of Fig. 7, there is a strong peak near 1280 cm^{-1}, arising from DMGaH.

ultimate stage in the process of replacing methyl groups by hydrogen atoms would, of course, be alane, AlH_3 (or more realistically its dimer, Al_2H_6). The existence of the corresponding gallium species Ga_2H_6 has very recently been demonstrated by Downs et al. [46], but alane has so far defied isolation, despite strenuous efforts. On the other hand, the trimethylamine adduct, trimethylamine alane (TMAA, $AlH_3 \cdot NMe_3$) is a reasonably volatile stable solid, and there has been considerable interest in this as a possible aluminium precursor. It has already been shown that AlGaAs films grown using mixtures of TMAA and TMGa at low pressures (eg. via MOMBE) show greatly reduced levels of carbon and oxygen contamination [47]: on the other hand, atmospheric pressure growth using these mixtures leads to AlGaAs in which carbon is still a major contaminant [48]. It would seem probable that gas-phase processes are responsible for this incorporation, a hypothesis borne out by evidence of deposition prior to the susceptor in atmospheric pressure growth [48]. We have therefore undertaken an investigation of gas-phase reactions in mixtures of both TMAA + TMGa [49] and TMAA + TEGa [50]. This was also of fundamental interest, since it was not known prior to this work whether adducts (such as TMAA) undergo exchange reactions to the same extent as the native parent compounds: certainly our experience with such adducts in solution suggested that exchange is considerably inhibited by adduct formation (see below).

Figures 1 and 2 of ref. 49 show a computer-added FTIR spectrum of TMAA +

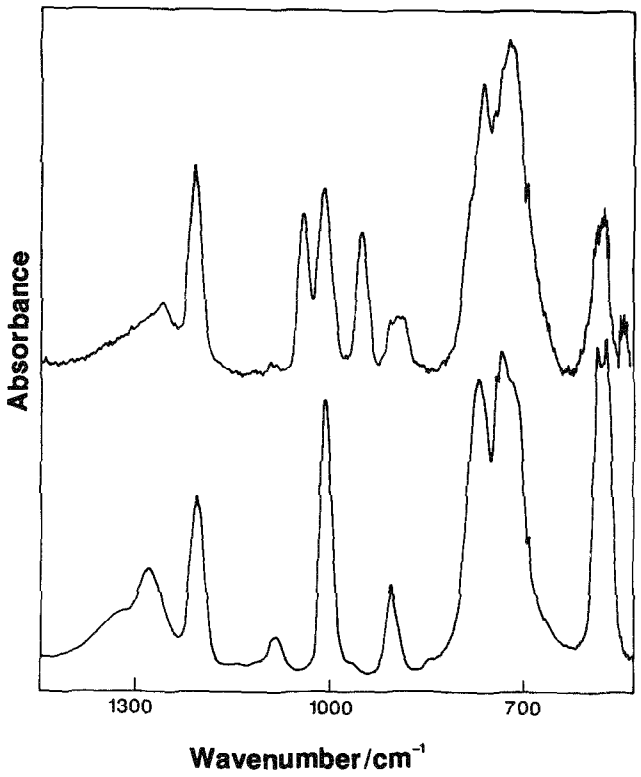

Fig. 10. As for Fig. 9, with DMAlD in place of DMAlH.

TMGa, and spectra of mixtures over a range of compositions. It is very evident that the mixtures contain species other than the two starting materials: indeed, except at extreme ratios of the two, no absorptions ascribable to either of the TMAA or TMGa starting materials were observable. At low TMAA:TMGa ratios, the principal constituents are free dimethyl gallium hydride, DMGaH [51], and trimethylamine complexed TMAl [52]. As the proportion of TMAA is increased, these species disappear, to be replaced by one or more trimethylamine-complexed gallium hydrides: although there are uncertainties in the reported spectra of $GaH_3 \cdot NMe_3$ [52], $MeGaH_2 \cdot NMe_3$ [53], and $Me_2GaH \cdot NMe_3$ [53], we have been able to identify these species by analogy with comparable spectra. Other features are ascribable to small amounts of $Me_2AlH \cdot NMe_3$ [54] and $Me_3Al \cdot NMe_3$ [32]. It is evident that hydrogen migrates preferentially to the more electronegative gallium centre, and the corresponding increase in methyl groups bound to aluminium explains the observation of carbon contamination [48]. It is also apparent that in the competition for limited NMe_3, the stronger Lewis acid aluminium is the winner, whatever its state of bonding to hydrogen or methyl groups.

These observations also explain a further negative feature of AlGaAs growth

using TMAA/TMGa mixtures. This is a considerable compositional non-uniformity of the grown layers, with an increase in aluminium in the downstream direction. This was somewhat unexpected, in the face of the known lower thermal stability of TMAA [55]. Figure 3 of ref. 49 shows FTIR spectra of a mixture of SF_6, TMAA, and TMGa subjected to IR LPHP. At low laser powers (temperatures), the most obvious change is loss of peaks identified with DMGaH: the only new gas-phase product observed is regeneration of TMGa (compare the observations of DMAlH). At higher powers, peaks due to metal–methyl bonds decay, with the appearance of methane in the gas phase. It is very evident that the gallium species resulting from the exchange reactions are more readily pyrolyzed first in this system, consistent with the results of the growth experiments.

We have also carried out similar studies using TMAA and TEGa [50]. This was of interest, since it is known that the use of TEGa results in considerably reduced carbon contamination. We have observed results similar to the TMAA+TMGa system. The interpretation of the results in this case is, however, complicated by two factors. The first is that many of the corresponding species formed by exchange reactions are of rather low volatility, and hence are not easily observed using straightforward gas-phase FTIR spectroscopy; the second is that some of the species produced by pyrolysis are also those formed by exchange, and it is difficult to disentangle these two in pyrolysis studies.

As an amusing postscript to the observations on mixtures of TMAA and trialkyl galliums, we have attempted to carry out a similar study of mixtures of TMAA and trimethyl indium, TMIn. This resulted in the immediate coating of the gas cell (and a portion of the vacuum line) with highly specular metallic In. Presumably similar exchange reactions, followed by immediate decomposition of the unstable resulting indium hydrides, are the cause. This may well be the first example of a room-temperature deposition of a metal from the gas phase in this kind of system: unfortunately, it seems likely to be of little practical value.

(v) IR LPHP of TMGa

As mentioned above, one of the principle problems arising from the use of aluminium precursors containing methyl groups (or of systems in which exchange reactions lead to such compounds) is the heavy incorporation of carbon. This is somewhat less of a problem in growth using TMGa, and is virtually absent in indium-containing layers using TMIn [2]. It might be tempting to relate this trend to the relative metal–methyl bond dissociation enthalpies in the series. However, this is debatable, since complete removal of methyl groups presumably involves the stages $MMe_3 \rightarrow MMe_2 \rightarrow MMe \rightarrow M$, and it is well known that these steps have very different activation energies [56]. Our observations on the homogeneous pyrolysis of TMAl (see above) have suggested that the predominant aluminium-containing radical is Me_2Al [14]. On the other hand, Price and his co-workers have interpreted kinetic

measurements of the pyrolysis of TMGa and TMIn [56] in terms of a slow removal of the first methyl group, followed by a much faster loss of the second. This would suggest that the predominant gas-phase metal-containing species would be GaMe. The other point here relates to the fate of the methyl radicals so produced. The major hydrocarbon products observed are methane and ethane, with the latter greatly increasing in significance with the atomic number of the metal [2]. Ethane is presumably formed by a third-body mediated recombination of methyl radicals, and its formation therefore effectively removes methyl radicals from the system. On the other hand, methane production must arise from hydrogen abstraction by methyl radicals, and since the only convenient source of hydrogen atoms (in the absence of hydrogen carrier gas) is the parent molecule, it follows that there is a significant production of species such as Me_2MCH_2. It is with this latter point in mind in particular that we have carried out a study of the IR LPHP of TMGa, and compared the results with that of TMAl [14].

Figure 11 shows the FTIR spectra of mixtures of TMGa and SF_6 subjected to IR LPHP. The only gas-phase product observed is methane. No gallium species corresponding to trapping of either Me_2Ga (cf. DMAlF in the case of TMAl [14]) or MeGa are observed; this is consistent with the lower Ga–F bond strength. The laser power required is lower than that for TMAl, as expected in the light of reports

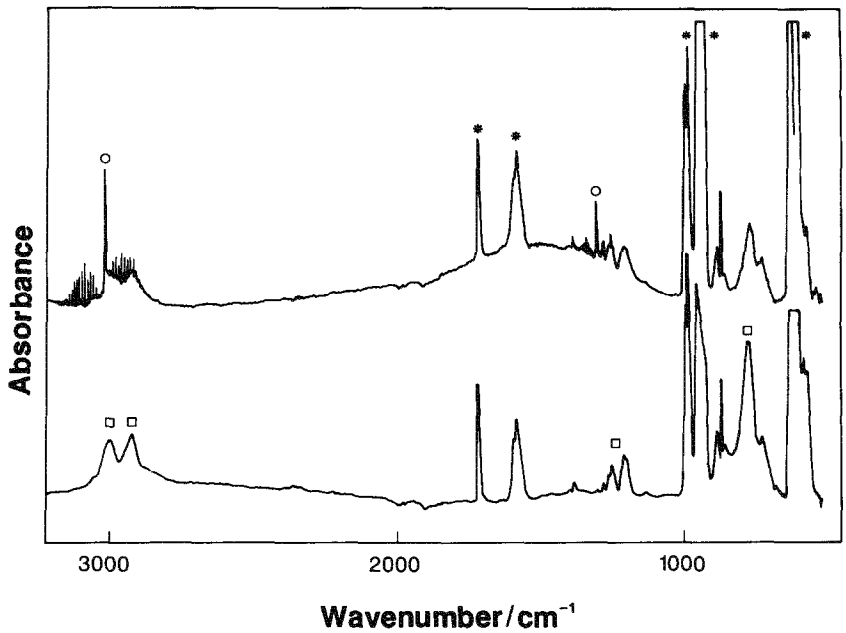

Fig. 11. FTIR spectra of a mixture of SF_6 (10 torr) and TMGa (2 torr) before (top) and after (bottom) exposure to 4 W IR laser irradiation for 120 s. Features identified arise from SF_6 (★), TMGa (□), and CH_4 (○). The broad background feature centred around 1500 cm^{-1} is a feature of TMGa pyrolysis, and is probably due to material deposited on the windows.

for the activation energies of the two pyrolyses [56]. As described above, the active constituents in MOCVD are often carried in a stream of a carrier gas, usually hydrogen, and we have therefore investigated the pyrolysis of TMGa and dTMGa in the presence of hydrogen or deuterium. The most significant result occurs in the mixture of TMGa and deuterium, illustrated in Fig. 12. Here substantial quantities of CH_3D are formed in addition to CH_4. In Fig. 13 is shown a graph of the ratio of CH_4:CH_3D produced against the ratio of initial pressures of TMGa and deuterium (in our experiments, the maximum pressure of deuterium is limited to about 10 torr); it is seen that the correlation is very good. This suggests a mechanism similar to that suggested above for TMAl, but in which there is competition between deuterium and TMGa for methyl radicals:

$$Me + TMGa \rightarrow CH_4 + Me_2GaCH_2 \tag{14}$$

$$Me + D_2 \rightarrow CH_3D + D \tag{15}$$

This result is in agreement with the studies of Larsen et al. [4,6], although here effects of surface reactions were not specifically eliminated. In the complementary isotopic system ($dTMGa + H_2$), the ratio of the product of abstraction from the carrier gas (CD_3H here) to that from the parent (CD_4) was much greater; this can be ascribed to the closely balanced activation energies for reactions (14) and (15),

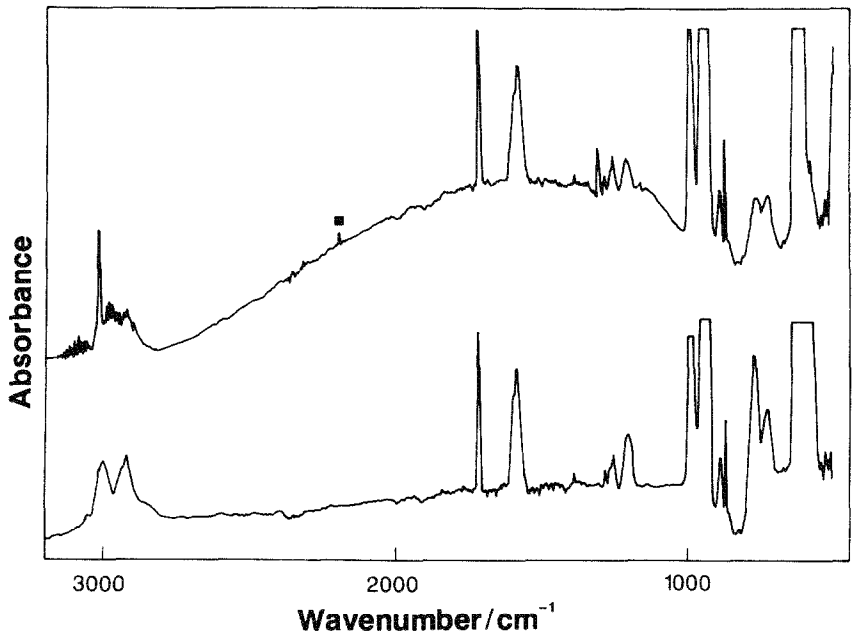

Fig. 12. As for Fig. 11 with the addition of 4 torr D_2. Note the appearance of CH_3D (marked ■) near 2200 cm^{-1}; since the intrinsic absorption of CH_3D is some 0.25 that of CH_4, the ratio of CH_3D:CH_4 is larger than apparent from the signal heights.

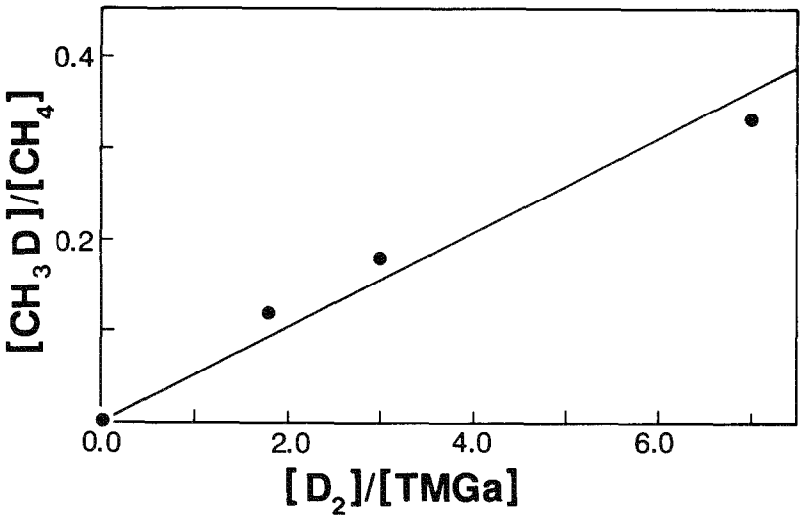

Fig. 13. Graph of ratio of CH_3D:CH_4 against ratio of D_2:TMGa in the IR LPHP of TMGa/D_2 mixtures. Because of uncertainties in the measurement of small signals, the error in the CH_3D:CH_4 ratio is estimated at about 10–20%.

and to the usual kinetic isotope effect. It is of interest to compare this with the case of TMAl, where the system corresponding to the latter (i.e. dTMAl + H_2) is the only one in which abstraction from the added gas is of importance. This difference results from the significantly lower C–H bond strength in TMAl [34].

(vi) IR LPHP of triethylgallium, TEGa

The heavy carbon contamination of deposited gallium or aluminium arising from methyl-containing sources has lead to the use of precursors containing higher alkyl groups. Unfortunately, TEAl has too low a vapour pressure to be of much value except in very-low-pressure (MOMBE) applications: on the other hand, it has been very widely demonstrated that use of TEGa leads to much purer GaAs than TMGa [2]. There has been some controversy over the mode of decomposition of TEGa in MOCVD, with some early work supporting a gallium alkyl homolysis [57]

$$TEGa \rightarrow Et_2Ga + Et \tag{16}$$

and more recent studies suggesting a β-elimination process [58]

$$TEGa \rightarrow Et_2GaH + C_2H_4 \tag{17}$$

These conclusions have been based entirely on observations of hydrocarbon products, (17) leading to production of ethene only, and (16) yielding products such as ethane and butane (as well as small amounts of ethene in disproportionation reactions). In no previous studies have gallium-containing products been reported,

nor has evidence for steps subsequent to (16) or (17) been adduced. This is a classic example of the situation where incomplete elimination of surface reaction can profoundly affect the course of reaction, since the radical mechanism (16) is likely to be much more significantly catalyzed than the β-elimination (17). Indeed, in a stirred flow reactor in an inert atmosphere of several hundred torr (designed specifically to reduce surface-catalyzed reaction) it was evident that such processes still dominated [59]. We have therefore undertaken an extensive investigation of the IR LPHP of TEGa [60–62].

The FTIR spectra of a mixture of TEGa and SF_6 before and after brief IR LPHP at modest laser power are shown in Fig. 1 of ref. 60. The most prominent feature of the product spectrum is the appearance of a strong broad absorption near 1640 cm^{-1}, together with sharp peaks readily ascribed to ethene. Examination of the pyrolysis cell revealed the presence of a liquid, and distillation from cell wall to window confirmed this liquid to be the origin of the broad absorption. The FTIR spectrum of this product, isolated by rapidly pumping away the volatile SF_6 and C_2H_4 product, is shown in Fig. 14; it is readily identified as diethylgallium hydride, DEGaH, in comparison with spectra of the similar DMGaH [51] and iBu_2GaH [63]. The broad absorption near 1640 cm^{-1} is very characteristic of Ga–H–Ga bridging bonds in a trimeric ring system. Very recently, Downs et al. have synthesised

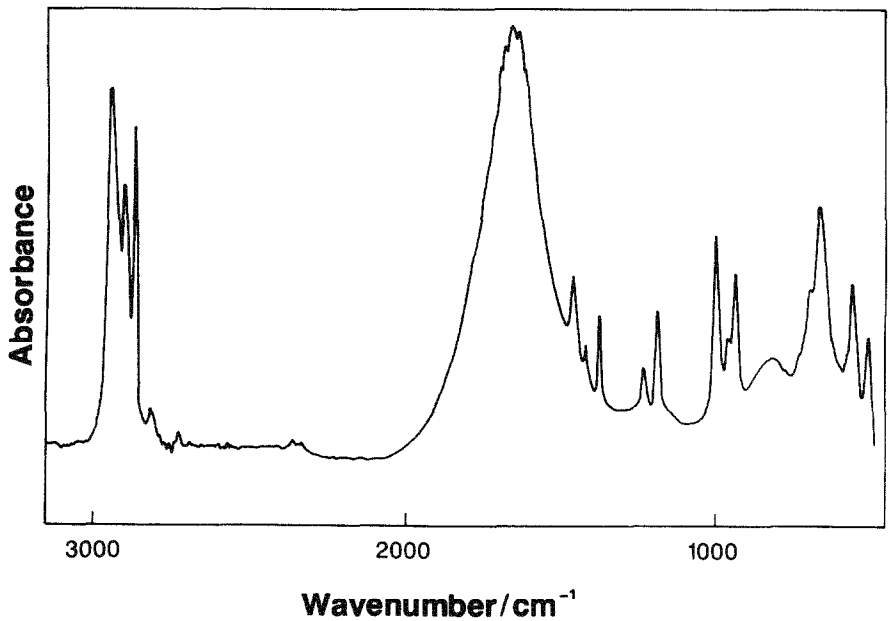

Fig. 14. FTIR spectrum of DEGaH, produced by IR LPHP of TEGa. The characteristic features of R_2GaH spectra are very evident, in particular the strong broad Ga–H antisymmetric (1640 cm^{-1}) and symmetric (800 cm^{-1}) stretching vibrations of the trimeric $\{Ga–H\}_3$ ring.

DEGaH by the reaction of Ga_2H_6 with C_2H_4 at high pressure [64], and the IR spectrum reported by them is identical with that of Fig. 14.

This identification was confirmed by ^1H NMR spectroscopy, a broad resonance at δH 3.07, typical of Ga–H, being observed at room temperature in $C_6D_5CD_3$. Although it proved possible to produce a sample of pure Et_2GaH by means of IR LPHP, the product often contained a proportion of unreacted TEGa or further products (of this, more later), and this complicates the interpretation of the NMR spectrum. On the other hand, this mixed system does provide a classic case of alkyl group exchange, as illustrated by the region of the ethyl group resonances at a series of temperatures, shown in Fig. 15. At −45°C, both CH_2 and CH_3 resonances of TEGa and DEGaH are clearly resolved, each exhibiting a $J(CH_2–CH_3)$ of 8 Hz; as the temperature is raised, these broaden and coalesce, and by room temperature the fast exchange limit is approached. On the other hand, there is little evidence of exchange between ethyl and hydride groups over this temperature range, although the Ga–H resonance broadens and shifts with increasing temperature.

On prolonged pyrolysis at low laser power, more ethene was produced, but although there were apparently changes in the region of the Ga–H vibration, they were obscured by its considerable width. The ^1H NMR spectrum of the product in this case revealed it to be apparently almost pure DEGaH. However, our experience with the mixtures of TMAA and TEGa described above suggested that details of the product might be more apparent on formation of adducts with NMe_3, and this was dramatically verified. The FTIR spectrum of the product of prolonged IR LPHP of

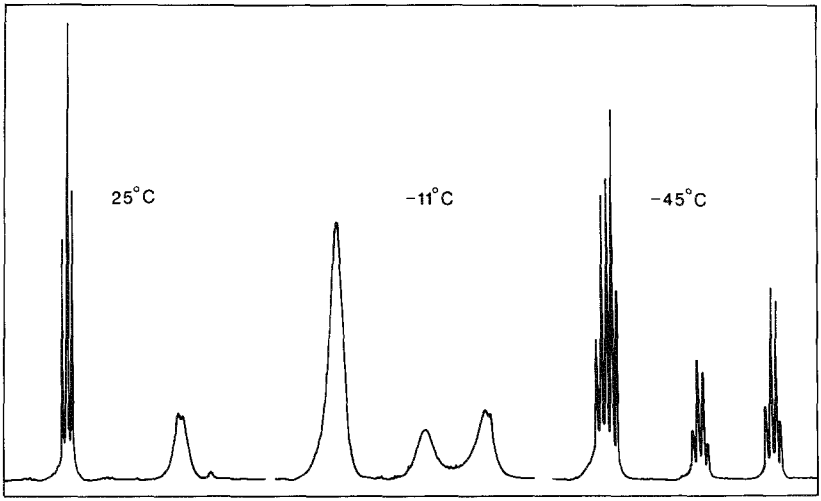

Fig. 15. ^1H NMR spectrum (300 MHz, 1.50–0.00 ppm) of a mixture of TEGa and DEGaH at various temperatures. At −45 °C, the higher field CH_3CH_2 quartet and CH_3CH_2 triplet of DEGaH are clearly distinguishable from those of TEGa, though overlapped in the latter case. At room temperature, the fast exchange limit has been reached for the CH_3CH_2 protons, and is approached for CH_3CH_2.

TEGa on addition of NMe_3 is shown in Fig. 16. The two sharp peaks in the region of terminal Ga–H stretches at 1798 and 1820 cm^{-1} are readily assigned to the adducts $Et_2GaH \cdot NMe_3$ and $EtGaH_2 \cdot NMe_3$ respectively, from our studies of TMAA + TEGa mixtures, and by analogy with the well-known corresponding methyl compounds [53]. Two bands assignable to the corresponding Ga–H bending modes are also observed at 820 and 752 cm^{-1}. The ^1H NMR spectrum of this adduct product provided the conclusive proof: the region of ethyl group CH_3CH_2 protons is especially informative, as shown in Fig. 17.

Here, quartets of singlets, doublets and triplets are readily assigned to the species $Et_3Ga \cdot NMe_3$, $Et_2GaH \cdot NMe_3$, and $EtGaH_2 \cdot NMe_3$; these spectra are of interest in their own right, since the coupling of 1.1 Hz provides the first example of ^3J coupling to a proton bound directly to gallium. Interestingly, in contrast with the native gallanes, in the adducts described here the only exchange observed at room temperature occurs between the Ga–H protons of the mono- and dihydride; evidently, adduct formation permits hydrogen atom exchange while preventing alkyl group transfer.

It is very evident that, under conditions of IR LPHP, the mechanism of the homogeneous pyrolysis of TEGa is almost exclusively β-elimination; only at very high laser powers have we observed any products attributable to a bond homolysis process (traces of butane). Furthermore, our observations suggest that the first β-elimination step (17) is readily followed by a second:

$$Et_2GaH \rightarrow EtGaH_2 + C_2H_4 \qquad (18)$$

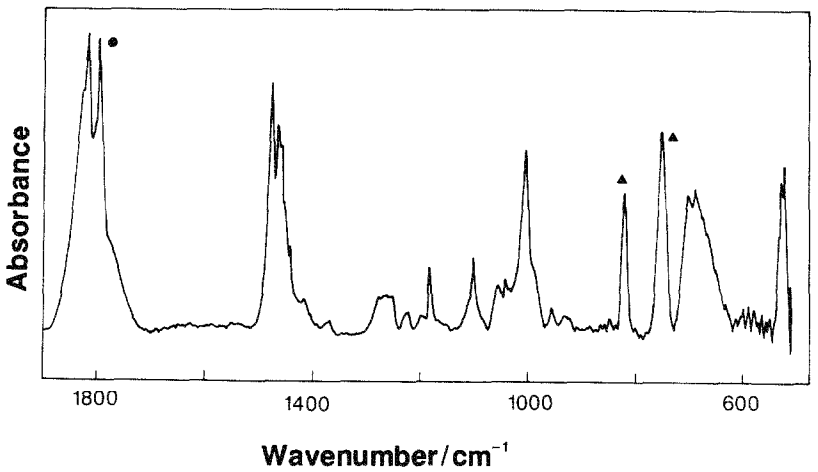

Fig. 16. FTIR spectrum of the result of adding NMe_3 to the products of prolonged IR LPHP of TEGa. As well as features arising from the NMe_3 and Et moieties, there are clearly two peaks (marked ●) near 1800 cm^{-1} in the region of terminal Ga–H stretches, and two near 800 cm^{-1} (▲) corresponding to Ga–H bending vibrations.

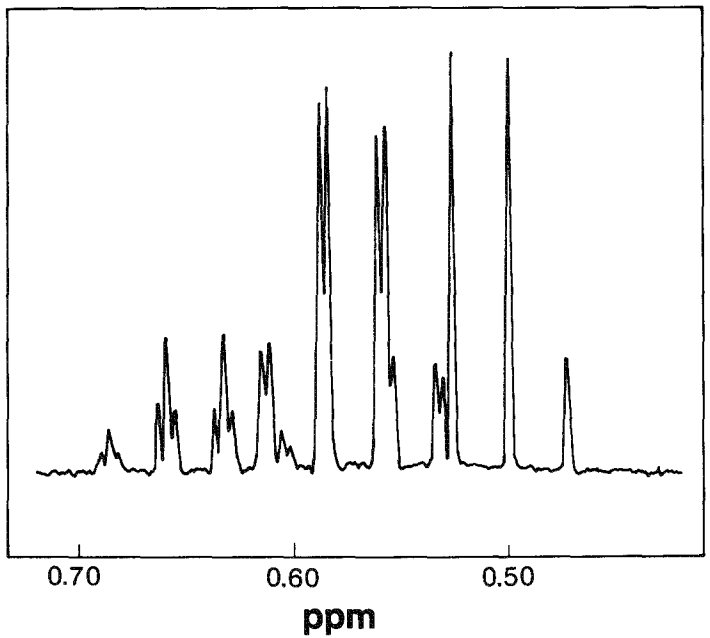

Fig. 17. ^{1}H NMR spectrum (300 MHz, 0.70–0.42 ppm, −60 °C) of the vapour whose FTIR spectrum is depicted in Fig. 16, condensed into d_8-toluene. See text for interpretation.

Our inability to produce a pure sample of $EtGaH_2$ is consistent with the known reversibility of reactions such as (17) and (18) in alkyl–aluminium systems [65], and with the demonstration of the double ethene insertion into Ga_2H_6 by Downs et al. [64]. This suggests that an equilibrium is attained in elimination of ethene, and that the completion of the deposition of gallium in MOCVD may require radical or surface processes. The hypothesis of this equilibrium is supported in recent preliminary observations in which almost complete elimination of ethyl groups has been attained by removal of the ethene product (see below).

(vii) IR LPHP of tributyl gallium compounds

The success of the study of TEGa described above has naturally led on to the study of other systems where β-elimination is possible. It has been suggested that this process may be less favoured in more sterically hindered systems, particularly if more stable radicals would be formed in homolysis processes: the obvious example here is tri-*tert*-butyl gallium (TBGa). Furthermore, there is considerable evidence that tri-iso-butyl gallium (IBGa) may be a lower-temperature source for gallium deposition than TEGa [66], and there is therefore considerable interest in its mode of pyrolysis. In both these cases, the vapour pressures of the starting materials are rather low, and we have therefore used a pyrolysis cell with a cylindrical hollow (see

Fig. 2) in these studies. This retains the starting material in the liquid form where it is not subject to direct pyrolysis; on the other hand, equilibration between liquid and vapour ensures the eventual reaction of all the liquid in the cell. It is probable that the evaporation of the liquid is the rate-limiting step in the pyrolysis in this situation. On the other hand, the process is still reasonably rapid, and it is very probable that this arrangement could be utilised in a large-scale synthesis of many of the products described in this review.

Figures 18 and 19 show FTIR spectra of the progress of IR LPHP in the two systems. In both cases, much lower laser power is required than for TEGa, and almost complete reaction is obtained in a matter of a few seconds. Once again, the by now characteristic Ga–H peaks near 1600 and 700 cm^{-1} are very apparent, confirming the formation of β-elimination products. Since these are relatively involatile, purification is readily achieved in these cases simply by rapidly pumping away the SF_6 photosensitiser and hydrocarbon product (2-methyl propene in both cases), leaving the spectra of essentially pure dibutyl gallium hydrides also shown in Figs. 19 and 20. On this occasion, however, there is evidence of features arising from the second β-elimination product, particularly in the *tert*-butyl case; thus an additional peak is observed near 650 cm^{-1} on longer pyrolysis. As in the case of TEGa, the

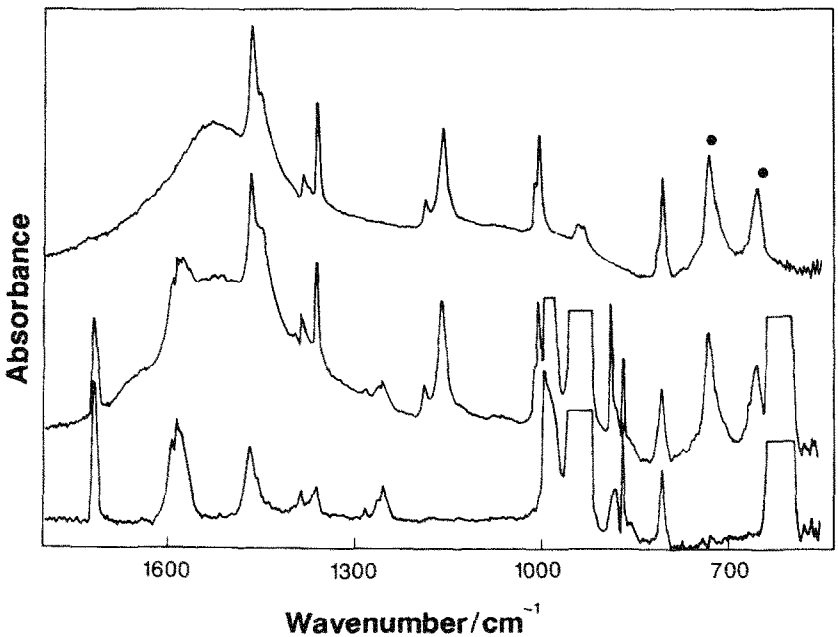

Fig. 18. FTIR spectra of a mixture of SF_6 (10 torr) and IBGa (as liquid in the cell hollow) before (bottom) and after (middle) exposure to 1.2 W IR laser power for 60 s. The top spectrum shows the FTIR spectrum of the product isolated as described in the text. Note the presence of two peaks (marked ●) in the Ga–H bending region near 700 cm^{-1}.

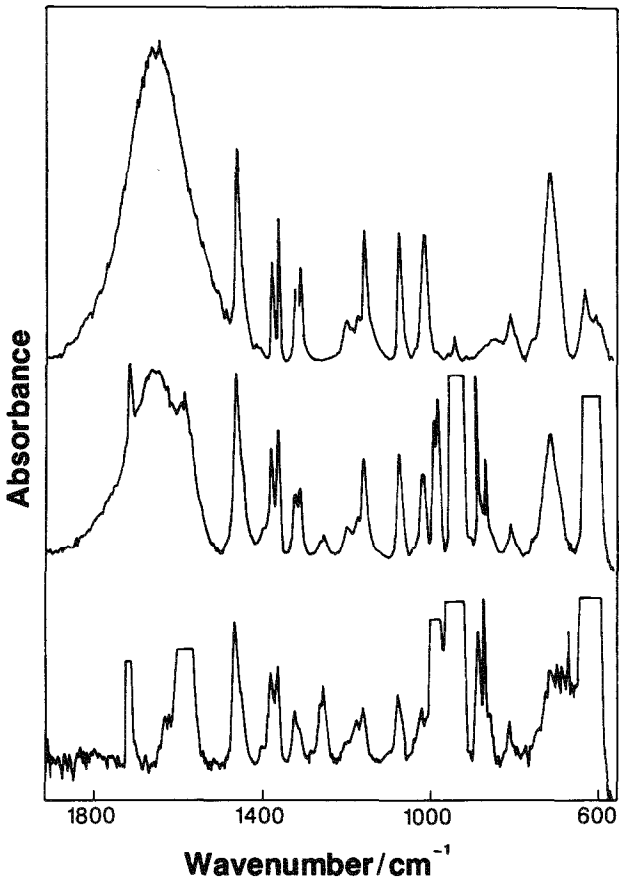

Fig. 19. As for Fig. 18 with TBGa in place of IBGa. In this case, evidence for two Ga–H bending peaks is less clear.

identification of the products was confirmed by ^{1}H NMR spectroscopy. That of the *tert*-butyl product is rather uninformative, since the singlet $C(CH_3)_3$ signals are not very sensitive to environment, but that of the iso-butyl compound at -60 °C is shown in Fig. 20. Here, in contrast with the TEGa system, features arising from both the monohydride and dihydride products are apparent in the region of the $Ga-CH_2CH(CH_3)_2$ and $Ga-CH_2CH(CH_3)_2$ resonances, although only a single Ga–H resonance is observed (presumably because of rapid exchange).

As in the case of TEGa, the formation of adducts with NMe_3 proved invaluable in confirming the identity of products. In the FTIR spectrum, the adducts exhibit sharper Ga–H terminal stretching vibrations as opposed to broad Ga–H–Ga bridging bands. In the ^{1}H NMR, exchange of all groups is slowed sufficiently (at -60 °C) that monohydride and dihydride Ga–H resonances become distinguishable, and ^3J H–Ga–C–H couplings are observable.

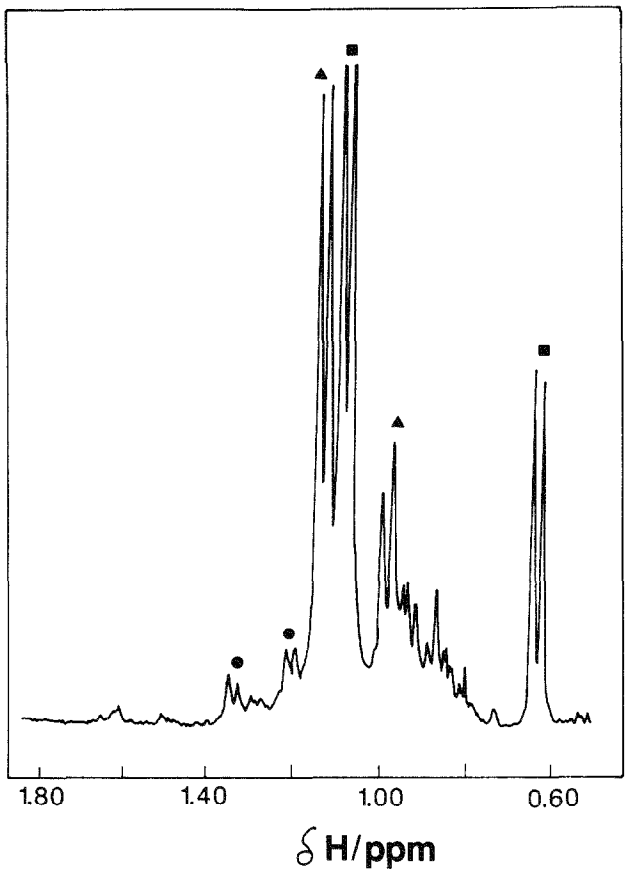

Fig. 20. ^{1}H NMR spectrum (300 MHz, 1.80–0.40 ppm, −60 °C) of the product whose FTIR spectrum is depicted in Fig. 19 (top), condensed into d_8-toluene. Only the region of $CH_2CH(CH_3)_2$ and $CH_2CH(CH_3)_2$ protons is shown: doublets (arising from coupling to $CH_2CH(CH_3)_2$) assignable to IBGa, iBu_2GaH, and $iBuGaH_2$ are marked ■, ▲, and ● respectively.

(viii) IR LPHP of mixtures of TMGa and TEGa

The techniques evolved for the study of the pyrolysis of TEGa, TBGa and IBGa have been put to use in mixed systems. This is of some interest, since there have been reports in the literature of the use of mixed Group III alkyl precursors. Thus Jones et al. have reported the use of dimethyl isobutyl aluminium [67], and Stringfellow and co-workers have described the advantages of dimethyl ethyl indium [68]. It was hoped that such compounds would exhibit the volatility of the methyl compounds, and the reduced carbon contamination characteristic of higher alkyl precursors. Our experience with such systems suggests that they do not retain their chemical integrity, and would in fact contain a more or less statistical mixture of all possible combinations. It also appeared that our IR LPHP technique would be

ideally suited to the study of such systems. We have therefore undertaken a study of the pyrolysis of mixtures of TEGa and TMGa as a model mixed system, in which the behaviour of the two constituents was well understood. The FTIR spectrum of equal pressures of TMGa and TEGa was compared with that of a computer co-added spectrum. It was immediately apparent from the region of Ga–Me and Ga–Et stretches that the mixture contained species other than the starting materials: although we have not undertaken a detailed analysis, it is very likely that these are simply exchange products such as $MeEt_2Ga$ and Me_2EtGa. It is significant that these exchange processes take place in the gas phase, and are quite rapid (much shorter than the 1 min or so required to acquire the spectra). It therefore seems that claims of isolation of pure heteroalkyl compounds should be treated with caution.

The results of pyrolysis of this mixture are shown in Fig. 21. At low laser powers, the only hydrocarbon evolved is ethene. At the same time, the characteristic trimeric Ga–H bridging vibration of DEGaH appears near 1640 cm^{-1}. On longer pyrolysis, this disappears, to be replaced by features of dimeric DMGaH near 1185 and 1280 cm^{-1} [51]. Eventually, these features also disappear, with the appearance of metallic gallium deposits. At no stage is any methane observed, in contrast with the DMAlH system. These observations are entirely in accord with the lower energy of activation for the β-elimination process: the overall effect is rapid loss of ethyl groups from the system, with the retention of methyl groups.

This latter is confirmed by ^1H NMR spectroscopy of the NMe_3 adducts of the

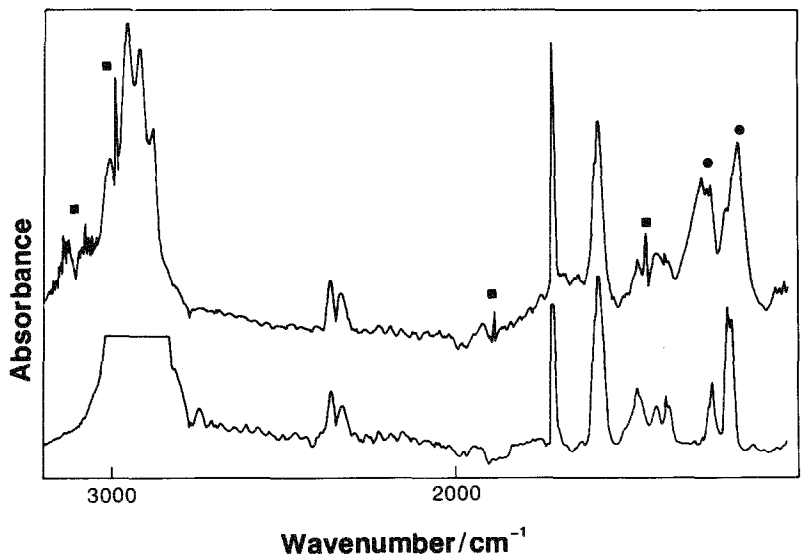

Fig. 21. FTIR spectra of a mixture of SF_6 (10 torr), TMGa (4 torr) and TEGa (4 torr) before (top) and after (bottom) exposure to 2 W IR laser irradiation for 5 min. Features due to C_2H_4 are marked ■, and to DMGaH ●. Note the lack of features due to DEGaH (compare Fig. 14) or CH_4 (compare Fig. 11).

products, prepared in the manner discussed above. A region of this spectrum of the products at an intermediate stage of pyrolysis is shown in Fig. 22.

The complete spectrum is very rich, showing a number of overlapped Ga–H resonances. On the other hand, in the region of hydrocarbon resonances, a large number of clearly identifiable species are observed. The methyl CH_3 region, shown in Fig. 22, is the most clearly resolved, showing six distinct species. Of these, three are non-hydrides (Me_3Ga, Me_2EtGa, and $MeEt_2Ga$), two are monohydrides (Me_2GaH and MeEtGaH), and the remaining one is the dihydride ($MeGaH_2$), all as NMe_3 adducts and exhibiting singlet, doublet or triplet splittings from Ga–H protons. Similarly, six ethyl-containing species are identifiable from the region of CH_3CH_2 resonances, although here the situation is complicated by overlap of the quartet structure arising from coupling to the ethyl CH_3CH_2 protons. In all, nine of the ten possible permutations of methyl, ethyl and hydrogen groups have been

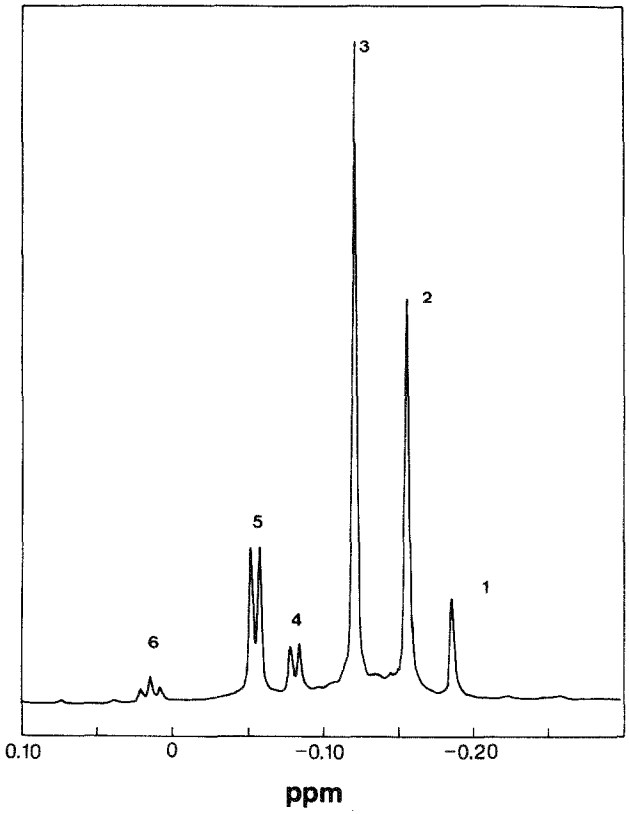

Fig. 22. ^1H NMR spectrum (300 MHz, 0.10 to −0.30 ppm, −60 °C) of the product of IR LPHP of a 1:1 mixture of TMGa and TEGa on addition of NMe_3 in d_8-toluene. Signals are assigned to methyl resonances in 1, $MeEt_2Ga \cdot NMe_3$; 2, $Me_2EtGa \cdot NMe_3$; 3, $Me_3Ga \cdot NMe_3$; 4, $MeEtGaH \cdot NMe_3$; 5, $Me_2GaH \cdot NMe_3$; and 6, $MeGaH_2 \cdot NMe_3$; the doublets or triplets arise from coupling to Ga–H protons.

identified—the only missing species is the gallane adduct $GaH_3 \cdot NMe_3$. As before, on warming to room temperature, all Ga–H resonances collapse into a single broad peak, and all couplings to Ga–H protons disappear; again, no evidence of exchange of alkyl groups in the adducts is observed.

E. CONCLUSIONS AND OUTLOOK

The studies described in detail in Sect. D have provided sufficient examples of the flavour of the work currently in progress at Leicester. It remains to draw together some of the threads, and to indulge in some modest crystal-ball gazing.

It was anticipated at the outset of the work that the unique advantages of the IR LPHP method would provide information about pyrolysis mechanisms inaccessible in other ways. This has been abundantly confirmed: in many cases, the information provided has considerably surpassed what might have been expected. The trapping of short-lived species, and the isolation of labile primary products, are perhaps the most novel observations; on the other hand, the unravelling of spectroscopic, structural, and dynamic detail has also been facilitated by the range of systems now studied.

For the future, an immediate priority is the ESR study of matrix-isolated pyrolysis products. This will certainly yield information not currently available, and should solve the thorny problem of the mechanism of DMAlH pyrolysis. A further project is the introduction of the Group V precursor (AsH_3, PH_3, etc.) into the system, with the application of the techniques evolved. Finally, there is the correlation of the properties of the deposited materials with the gas-phase mechanisms elucidated. For this, cooperative studies with surface scientists will be invaluable, and this has already been initiated [69].

It is apparent from the foregoing that what started out as a project limited to the investigation of pyrolysis reaction mechanisms has spilled over into a wide range of related areas. The organometallic chemistry of aluminium and gallium is particularly rich, principally because of the many complexities arising from bridging, exchange and adducting reactions. The studies described here have provided a glimpse of one of the more fascinating areas of main group coordination chemistry, and have demonstrated once again the benefits of bringing novel experimental methods to bear on the study of familiar systems.

ACKNOWLEDGEMENTS

It is a pleasure to acknowledge the considerable contribution of the Science and Engineering Research Council to this work in the shape of grants for the purchase of equipment, post-doctoral research fellowships, and studentships. A number of people have made invaluable contributions (both material and scientific). Dr. Tony Jones of Epichem Ltd., has provided most of the chemicals, Dr. Peter

Wright and Professor Brian Cockayne of RSRE, Malvern, have shown enthusiastic support for the entire project, and my colleagues Iain Davidson, Ray Kemmitt, Tom Claxton and Barrie Raynor have always been willing to provide advice in those areas where my ignorance was apparent. My greatest debt, however, is to those who have carried out most of the experiments: post-doctoral fellows Shakher Puntambekar and Ross Markwell, graduate students Ghalib Atiya, David Pape, Andy Grady, and Rachel Linney, and the many final-year undergraduates whose names appear in the references.

REFERENCES

1 S.J. Moss and A. Ledwith (Eds.), The Chemistry of the Semiconductor Industry, Blackie, Glasgow, 1987.
2 G.B. Stringfellow, Organometallic Vapor-phase Epitaxy: Theory and Practice, Academic Press, San Diego, 1989.
3 H.M. Manasevit, Appl. Phys. Lett., 12 (1968) 156.
4 C.A. Larsen, N.I. Buchan, S.H. Li and G.B. Stringfellow, J. Cryst. Growth, to be published.
5 J.E. Butler, N. Bottka, R.S. Sillmon, and D.K. Gaskill, J. Cryst. Growth, 77 (1986) 163.
6 C.A. Larsen, N.I. Buchan and G.B. Stringfellow, Appl. Phys. Lett., 52 (1988) 480.
7 A.S. Grady, PhD Thesis, University of Leicester, 1991.
8 A.P. Ashworth, E.N. Clark and P.G. Harrison, J. Chem. Soc. Chem. Commun., (1987) 782; Trans. Faraday Soc., 86 (1990) 4059.
9 D.K. Russell, Chem. Soc. Rev., 19 (1990) 407.
10 W.M. Shaub and S.H. Bauer, Int. J. Chem. Kinet., 7 (1975) 509.
11 G.A. Atiya, D.A. Pape and D.K. Russell, unpublished results.
12 F.W. Lampe and J. Biedzycki, Spectrochim. Acta Part A, 46 (1990) 631.
13 K.A. Holbrook, G.A. Oldershaw and M. Matthews, Int. J. Chem. Kinet., 17 (1985) 1275.
14 G.A. Atiya, A.S. Grady, S.A. Jackson, N. Parker and D.K. Russell, J. Organomet. Chem., 378 (1989) 307.
15 M. Suzuki and M. Sato, J. Electrochem. Soc. Solid State Sci. Technol., 132 (1985) 1684.
16 N. Suzuki, C. Anayama, K. Masu, T. Tsubouchi and N. Mikoshiba, Jpn. J. Appl. Phys., 25 (1986) 1236.
17 D.B. Chambers, G.E. Coates, F. Glockling and M. Weston, J. Chem. Soc. A, (1969) 1712.
18 J. Pola, J.M. Bellama and V. Chvalovsky, Collect. Czech. Chem. Commun., 46 (1981) 3088.
19 R.C. Weast (Ed.), Handbook of Chemistry and Physics, Chemical Rubber Publishing Co. Press, Boca Raton, 60th edn., 1980.
20 J.J. Eisch, in G. Wilkinson, F.G.A. Stone and E.W. Abel (Eds.), Comprehensive Organometallic Chemistry, Vol. 1, Pergamon Press, Oxford, 1982, Chap. 6.
21 E.G. Hoffmann, Z. Elektrochem., 64 (1960) 614.
22 E.G. Hoffmann, Trans. Faraday Soc., 58 (1962) 642.
23 C.H. Henrickson and D.P. Eyman, Inorg. Chem., 6 (1967) 1461.
24 G.A. Atiya, A.S. Grady, D.K. Russell and T.A. Claxton, Spectrochim. Acta Part A, 47 (1991) 467.
25 S. Kvisle and E. Rytter, Spectrochim. Acta Part A, 40 (1984) 939.
26 J.B. Raynor, K. Mach and D.K. Russell, unpublished results.
27 D.W. Squire, C.S. Dulcey and M.C. Lin, J. Vac. Sci. Technol. B, 3 (1985) 1513.
28 T.A. Claxton, personal communication, 1991.

29 D.J. Fox, D. Ray, P.C. Rubesin and H.F. Schaefer III, J. Chem. Phys., 73 (1980) 3246.
30 A.S. Grady, R.D. Markwell, D.K. Russell and P.J. Wright, work in progress.
31 T. Wartik and H.I. Schlesinger, J. Am. Chem. Soc., 75 (1953) 835.
32 E.G. Hoffmann and G. Schomburg, Z. Elektrochem., 61 (1957) 1101, 1110.
33 H.W. Schrötter and E.G. Hoffmann, Ber. Bunsenges. Phys. Chem., 68 (1964) 627.
34 A.S. Grady, S.G. Puntambekar and D.K. Russell, Spectrochim. Acta, Part A, 47 (1991) 47.
35 A. Almenningen, G.A. Anderson, F.R. Forgaard and A. Haaland, Acta. Chem. Scand., 26 (1972) 2315.
36 R. Bhat, M.A. Koza, C.C. Chang, S.A. Schwartz and T.D. Harris, J. Cryst. Growth, 77 (1986) 7.
37 A.S. Grady, S.G. Puntambekar and D.K. Russell, in preparation.
38 A.S. Grady, R.E. Linney and D.K. Russell, unpublished work.
39 M. Fishwick, C.A. Smith and M.G.H. Wallbridge, J. Organomet. Chem., 21 (1970) P9.
40 A.S. Grady, R.E. Linney and D.K. Russell, unpublished results.
41 M.P. Coogan, A.S. Grady, M.D. Robertson and D.K. Russell, unpublished results.
42 J.P. Oliver, Adv. Organomet. Chem., 15 (1977) 235.
43 E.A. Jeffery and T. Mole, Aust. J. Chem., 26 (1973) 739.
44 A.S. Grady, R.E. Linney, M. Jones and D.K. Russell, unpublished work.
45 J.J. Eisch and S.G. Rhee, J. Organomet. Chem., 42 (1972) C73.
46 A.J. Downs, M.J. Goode and C.R. Pulham, J. Am. Chem. Soc., 111 (1989) 1936.
47 C.R. Abernathy, A.S. Jordan, S.J. Pearton, W.S. Hobson, D.A. Bohling and G.T. Muhr, Appl. Phys. Lett., in press.
48 J.S. Roberts, C.C. Button, J.P.R. David, A.C. Jones and S.A. Rushworth, J. Cryst. Growth, 104 (1990) 857.
49 A.S. Grady, R.D. Markwell, D.K. Russell and A.C. Jones, J. Cryst. Growth, 106 (1990) 239.
50 A.S. Grady, R.D. Markwell, D.K. Russell and A.C. Jones, J. Cryst. Growth, 110 (1991) 739.
51 P.L. Baxter, A.J. Downs, M.J. Goode, D.W.H. Rankin and H.E. Robertson, J. Chem. Soc. Dalton Trans., (1990) 2873.
52 N.N. Greenwood, A. Storr and M.G.H. Wallbridge, Inorg. Chem., 2 (1963) 1036.
53 A. Storr and V.G. Wiebe, Can. J. Chem., 47 (1969) 673.
54 O.T. Beachley, Jr. and J.D. Bernstein, Inorg. Chem., 12 (1963) 183.
55 A.C. Jones, S.A. Rushworth, P.A. Bohling and G.T. Muhr, J. Cryst. Growth, 106 (1990) 246.
56 M.G. Jacko and S.J.W. Price, Can. J. Chem., 41 (1963) 1560.
57 M.C. Paputa and S.J.W. Price, Can. J. Chem., 57 (1979) 3178.
58 P.W. Lee, T.R. Omstead, D.R. McKenna and K.F. Jensen, J. Cryst. Growth, 85 (1987) 165.
59 I.M.T. Davidson and S.G. Puntambekar, personal communication, 1991.
60 A.S. Grady, A.L. Mapplebeck, D.K. Russell and M.G. Taylorson, J. Chem. Soc. Chem. Commun., (1990) 929.
61 A.S. Grady, R.D. Markwell and D.K. Russell, J. Chem. Soc. Chem. Commun., (1991) 14.
62 A.S. Grady, R.D. Markwell and D.K. Russell, J. Chem. Soc. Dalton Trans., submitted for publication.
63 V.V. Markova, V.A. Kormer and A.A. Petrov, J. Gen. Chem. USSR (Engl. Transl.), 37 (1967) 1662.
64 A.J. Downs, M.J. Goode and C.R. Pulham, J. Am. Chem. Soc., 113 (1991) 5149.
65 Ref. 20 and references cited therein.
66 A.C. Jones, personal communication, 1991.
67 A.C. Jones, P.R. Jacobs, S.A. Rushworth, J.S. Roberts, C. Button, P.J. Wright, P.E. Oliver and B. Cockayne, J. Cryst. Growth, 96 (1989) 769.

68 K.L. Fry, C.P. Kuo, C.A. Larsen, R.M. Cohen, G.B. Stringfellow and A. Melas, J. Electron. Mater., 15 (1986) 91.
69 J.S. Foord and A.C. Jones, personal communication, 1991.

APPENDIX

The growth processes described in the preceding pages have been accorded a number of acronyms. We have preferred metal organic chemical vapour deposition (MOCVD), avoiding any preconceptions over the nature of the deposition implied by metal organic vapour phase epitaxy (MOVPE). Other authors have designated the precursors organo-metallic, yielding OMCVD and OMVPE. The corresponding molecular beam epitaxy becomes MOMBE; this takes place at very low pressures of precursors, and is undoubtedly heterogeneous.

The precursor acronyms used here have found wide acceptance; we have had to coin abbreviations in the same vein for variously deuterated or otherwise substituted variations. The following list encompasses those found in the text.

TMAl	trimethyl aluminium (trimethylalane), $(CH_3)_3Al$
dTMAl	fully deuterated TMAl, $(CD_3)_3Al$
TMGa	trimethyl gallium (trimethylgallane), $(CH_3)_3Ga$
dTMGa	fully deuterated TMGa, $(CD_3)_3Ga$
TMIn	trimethyl indium, $(CH_3)_3In$
TEGa	triethyl gallium (triethylgallane), Et_3Ga
TBGa	tri-*tert*-butyl gallium, tBu_3Ga
IBGa	tri-iso-butyl gallium, iBu_3Ga
DMAlH	dimethyl aluminium hydride (dimethylalane), $(CH_3)_2AlH$
DMAlD	dimethyl aluminium deuteride, $(CH_3)_2AlD$
d_6-DMAlH	di(perdeuteromethyl)alane, $(CD_3)_2AlH$
DMGaH	dimethyl gallium hydride (dimethylgallane), $(CH_3)_2GaH$
DEGaH	diethyl gallium hydride (diethylgallane), Et_2GaH
DMAlF	dimethyl aluminium fluoride, $(CH_3)_2AlF$
TMAA	trimethylamine alane, $AlH_3 \cdot NMe_3$